ARTICLE IN PRESS

Journal of Computational Physics xxx (2008) xxx–xxx

Contents lists available at ScienceDirect

Journal of Computational Physics

journal homepage: www.elsevier.com/locate/jcp

Boundary integral solutions of coupled Stokes and Darcy flows

Svetlana Tlupova [a,*], Ricardo Cortez [b]

[a] Department of Mathematical Sciences and Center for Applied Mathematics and Statistics, New Jersey Institute of Technology, 323 Dr. Martin Luther King, Jr. Boulevard, University Heights, Newark, NJ 07102, USA
[b] Department of Mathematics, Tulane University, 6823 St. Charles Avenue, New Orleans, LA 70118, USA

ARTICLE INFO

Article history:
Received 18 March 2008
Received in revised form 29 July 2008
Accepted 2 September 2008
Available online xxxx

Keywords:
Boundary integral method
Stokes flow
Darcy's equations
Regularized Stokeslets

ABSTRACT

An accurate computational method based on the boundary integral formulation is presented for solving boundary value problems for Stokes and Darcy flows. The method also applies to problems where the equations are coupled across an interface through appropriate boundary conditions. The adopted technique consists of first reformulating the singular integrals for the fluid quantities as single and double layer potentials. Then the layer potentials are regularized and discretized using standard quadratures. As a final step, the leading term in the regularization error is eliminated in order to gain one more order of accuracy. The numerical examples demonstrate the increase of the convergence rate from first to second order and show a decrease in magnitude of the error. The coupled problems require the computation of the gradient of the Stokes velocity at the common interface. This boundary condition is also written as a combination of single and double layer potentials so that the same approach can be used to compute it accurately. Extensive numerical examples show the increased accuracy gained by the correction terms.

1. Introduction

In this paper we present a numerical method for solving problems of free fluid flow coupled with a porous medium flow. These arise in many industrial applications, such as filtration, oil recovery, fluid flow though body tissues [40], the remediation of soils by means of bacterial colonies [2]. We consider the model of Stokes equations in the fluid region coupled across a fixed interface with Darcy's equations in the porous region. In this setting, the governing equations have different orders in different regions and the interface conditions that couple the flows have to be chosen carefully.

Obtaining analytical solutions is not feasible for general problems with complex geometries, so various numerical methods have been developed, mostly based on the domain decomposition method and the finite element method ([17,28,22,33,10,20,21,34]). There also have been attempts to deal with similar problems with the use of fundamental solutions and boundary integral methods ([18,41,9]).

Our objective is to develop a method based on the boundary integral formulation for computing the fluid/porous medium problem with high accuracy using fundamental solutions of Stokes and Darcy's equations. The boundary integral formulation is a natural approach for viscosity-dominated flows. In this formulation, the solutions are represented as integrals over the boundaries, so the dimension of the computation reduces by one. This is advantageous for problems with large domains, exterior domains, and situations where the boundary may have a complicated nature, since only the boundary has to be discretized. The difficulty arises in the singularities in the integrands. A natural approach to deal with singular integrals is to regularize the integrands and discretize the integrals by a simple quadrature. We use the regularization method proposed

* Corresponding author.
E-mail addresses: stlupova@njit.edu (S. Tlupova), cortez@math.tulane.edu (R. Cortez).

0021-9991/$ - see front matter © 2008 Elsevier Inc. All rights reserved.
doi:10.1016/j.jcp.2008.09.011

Please cite this article in press as: S. Tlupova, R. Cortez, Boundary integral solutions of coupled Stokes and Darcy flows, J. Comput. Phys. (2008), doi:10.1016/j.jcp.2008.09.011

for Stokes flow by Cortez in [14] to approximately evaluate the integrals. The regularization error in the method is analyzed and a correction to eliminate the leading order term is derived. This has been done previously for the case of Stokes flow alone but not for Darcy's law or for the coupled Stokes–Darcy problem. When the evaluation point is near the boundary, the integrals are nearly singular. This causes traditional quadrature techniques with a fixed number of nodes to give inaccurate results. Our main goal is then to increase the accuracy, which is especially critical for the boundary conditions at the interface, where the derivative of velocity is needed. Corrections advance the accuracy of the method to the next order. As our results show, this is true for all fluid quantities in both domains and across the interface.

1.1. The model equations

Stokes flows appear in many applications where the fluid viscosity is high and/or the velocity and length scales are small. In dimensional form, the steady state equations are

$$0 = -\nabla p + \mu\Delta\mathbf{u} + \mathbf{f}, \tag{1}$$

$$\nabla \cdot \mathbf{u} = 0, \tag{2}$$

where p is the pressure, $\mathbf{u}$ is the velocity vector, and $\mathbf{f}$ is the external force per unit volume.

On the macroscopic scale, a porous medium can be described by a model where the solid and the fluid occupy the entire volume. The medium is regarded as a homogeneous domain and modeled as a continuum where a representative volume element is larger than the average pore size but much smaller than the length scale of the system. For this model of saturated flow in homogeneous porous media, the balance of momentum is given by Darcy's law:

$$\mathbf{u} = -\frac{K}{\mu}\nabla p,$$

where $\mathbf{u}$ and p are the (averaged) fluid velocity and hydrostatic pressure, μ is the fluid dynamic viscosity, and K is the permeability of the porous medium. The last quantity depends on the structure of the solid matrix. We will assume that the medium is isotropic, $K = kI$, where k is an averaged quantity that encodes the information about the pore structure, although this assumption is not essential. Since in the Darcy's equations viscous stresses on the fluid are neglected and only the damping force of the porous medium is considered, it is valid for small permeabilities. See, for example, [7,36,45].

1.2. Interface conditions

The flow region that contains both Stokes and Darcy flows requires a careful coupling of these different systems at the interface through appropriate boundary conditions. One condition is continuity of the normal components of velocity,

$$\mathbf{u}_S \cdot \hat{n} = \mathbf{u}_D \cdot \hat{n}.$$

Here we denote the Stokes quantities by subscript S and Darcy quantities by subscript D. This condition represents mass conservation across the interface, but it is not sufficient in order to have a fully described system. Since we are considering a viscous model, a condition on the tangential component of velocity is needed. The condition classically imposed was zero tangential velocity along the interface. But as noted in [28] for example, this condition was not in good agreement with experimental observations. It is valid at an impermeable boundary and is not suitable at a naturally permeable wall.

Assumptions that are accepted in the derivation of Darcy's law, like the periodicity of the porous medium, or its homogeneity, break down near boundaries. Effective boundary conditions need to be formulated to account for the boundary layers near the interfaces. The condition widely accepted was derived experimentally by Beavers and Joseph [8] and verified rigorously by Saffman [42]. It states that the difference between the tangential components of the free fluid velocity and the filtration velocity is proportional to the shear stress from the free fluid and the proportionality constant depends linearly on the square root of the permeability,

$$\frac{\partial u_S^{(\tau)}}{\partial \hat{n}} = \frac{\gamma}{\sqrt{k}}(u_S^{(\tau)} - u_D^{(\tau)})$$

along the interface between the two regions. Here, as before, k is the permeability of the isotropic medium and γ is a dimensionless slip coefficient that depends on the geometry of the porous medium. $u^{(\tau)}$ is the tangential velocity and $\hat{n}$ is the unit normal vector that points out of the region of free flow and into the porous region.

According to the condition of Beavers and Joseph, the velocity across the interface does not have to be continuous, and the magnitude of the slip is directly proportional to the shear stress. In his study of this condition, Saffman in [42] used a statistical approach to show that the Darcy velocity is $O(k)$ relative to the Stokes velocity and proposed a modification with the Darcy term omitted,

$$\frac{\partial u_S^{(\tau)}}{\partial \hat{n}} = \frac{\gamma}{\sqrt{k}}u_S^{(\tau)}. \tag{3}$$

Please cite this article in press as: S. Tlupova, R. Cortez, Boundary integral solutions of coupled Stokes and Darcy flows, J. Comput. Phys. (2008), doi:10.1016/j.jcp.2008.09.011

This is the condition we use in this paper. The third condition we use at the interface is continuity of normal component of the normal stress:

$$p_S - 2\mu\hat{n}\cdot\mathbf{D}_S\cdot\hat{n} = p_D,$$

where $\mathbf{D}_S = \frac{1}{2}[\nabla\mathbf{u}_S + (\nabla\mathbf{u}_S)^T]$ is the Stokes deformation tensor. This condition allows the pressure to be discontinuous. The numerical solution proposed in this work approximates all the fluid quantities to the same accuracy, thus allowing for implementation of continuity of pressure as well, when it is more appropriate. For discussion on the coupling conditions we refer to Jager and Mikelić [25], Layton et al. [28], Discacciati et al. [17].

1.3. Boundary integral formulation of Stokes flow

The fundamental solutions form the basis of the boundary integral methods that are used to construct solutions of general boundary value problems. The fundamental solution of (1) and (2), or the Stokeslet, is associated with a singular point force of strength $\mathbf{f}_0$ concentrated at a point $\mathbf{x}_0$ in free space,

$$\mathbf{f}(\mathbf{x}) = \mathbf{f}_0\delta(\mathbf{x}-\mathbf{x}_0),$$

where $\delta(\mathbf{x})$ is the two- or three-dimensional Dirac delta function. The pressure and velocity associated with the Stokeslet have the following well-known expressions ([14])

$$p(\mathbf{x}) = \mathbf{f}_0\cdot\nabla G(\mathbf{x}-\mathbf{x}_0),$$

$$\mu\mathbf{u}(\mathbf{x}) = -\mathbf{f}_0 G(\mathbf{x}-\mathbf{x}_0) + (\mathbf{f}_0\cdot\nabla)\nabla B(\mathbf{x}-\mathbf{x}_0),$$

where G and B are solutions of $\Delta G(\mathbf{x}) = \delta(\mathbf{x})$ and $\Delta B(\mathbf{x}) = G(\mathbf{x})$ in free space:

$$G(\mathbf{x}) = \frac{1}{2\pi}\ln|\mathbf{x}|, \quad B(\mathbf{x}) = \frac{|\mathbf{x}|^2}{8\pi}(\ln|\mathbf{x}|-1) \quad \text{in } \mathbb{R}^2$$

and

$$G(\mathbf{x}) = -\frac{1}{4\pi|\mathbf{x}|}, \quad B(\mathbf{x}) = -\frac{|\mathbf{x}|}{8\pi} \quad \text{in } \mathbb{R}^3.$$

The superposition of Stokeslets and their derivatives, which represent other, more singular solutions of Stokes equations, are used to construct models for many applications in areas like slender body theory, flagellar hydrodynamics, lubrication theory, and numerous others ([11,29–31,26,32,24,23,37–39,43,16]).

In cases when the body force is applied on the surface of a fluid volume, a boundary integral formulation represents the Stokes velocity and pressure as integrals over the boundaries, so the problem reduces its dimensionality. For a given set of boundary conditions, we can represent both solutions as singular integrals. For example, for Stokes flow in a region Ω with boundary given by $\mathbf{x}(s)$, $0 \leqslant s \leqslant L$, we can write the solution as

$$p(\mathbf{x}) = \int_0^L \mathbf{f}(s)\cdot\nabla G(\mathbf{x}-\mathbf{x}(s))\mathrm{d}s, \tag{4}$$

$$\mu\mathbf{u}(\mathbf{x}) = \int_0^L \{-\mathbf{f}(s)G(\mathbf{x}-\mathbf{x}(s)) + (\mathbf{f}(s)\cdot\nabla)\nabla B(\mathbf{x}-\mathbf{x}(s))\}\mathrm{d}s, \tag{5}$$

where the force $\mathbf{f}$ is distributed along the boundary $\partial\Omega$. Imposing velocity boundary conditions results in solving integral equations of the first or second kind for the unknown force. The difficulty of this formulation is in the singularities in the integrands. As presented in this paper, we can regularize the kernels and discretize the integrals by a quadrature. But as the evaluation point $\mathbf{x}$ approaches a boundary point $\mathbf{x}(s)$, the integrals become nearly singular, and without further modifications traditional integration quadratures do not give the desired accuracy. The integrals for Stokes flow in a closed domain in two dimensions were computed with high accuracy in [14,6].

The integral in (5) is continuous across the boundary, but the integral in (4) is more singular and has different limiting values on either side of the boundary which are different from the value on the boundary itself. Thus, for this pressure representation, some modifications are required to account for the jump conditions at the boundary in an interior/exterior problem. In a coupled Stokes–Darcy problem, the interface condition (3) requires accurate computation of the velocity gradients. Although the velocity representation (5) is continuous, the derivative of the integral will have a jump across the boundary of the domain. Therefore, similarly to pressure, when the velocity gradients are needed on the boundary, certain jump conditions have to be incorporated into the solution. In addition, the singularities in the kernels increase with each differentiation, and this presents additional difficulties in the management of singular and nearly singular integrals. In Section 3.2, we give the integral representation for velocity derivatives, which is then regularized. This allows us to reduce the error by adding a correction term. The correction takes care of the jump at the boundary automatically.

Please cite this article in press as: S. Tlupova, R. Cortez, Boundary integral solutions of coupled Stokes and Darcy flows, J. Comput. Phys. (2008), doi:10.1016/j.jcp.2008.09.011

1.4. Boundary integral formulation of Darcy flow

The Darcy equations are linear as well. Therefore, we find the fundamental solution by solving

$$\frac{\mu}{k}\mathbf{u} = -\nabla p + \mathbf{g}_0\delta(\mathbf{x}-\mathbf{x}_0),$$
$$\nabla\cdot\mathbf{u} = 0.$$

Then it can be integrated over the boundary of the flow region Ω to obtain

$$p(\mathbf{x}) = \int_0^L \mathbf{g}(s)\cdot\nabla G(\mathbf{x}-\mathbf{x}(s))\mathrm{d}s, \tag{6}$$

$$\mu\mathbf{u}(\mathbf{x}) = -k\int_0^L (\mathbf{g}(s)\cdot\nabla)\nabla G(\mathbf{x}-\mathbf{x}(s))\mathrm{d}s. \tag{7}$$

The Darcy pressure has the same expression as the Stokes pressure, but kernels in the Darcy velocity are more singular than the Stokeslet, making it more difficult to obtain high accuracy in the numerical computation of the integrals.

2. Numerical method

2.1. Regularization and error

In many situations it is desirable to smooth out the singularity in the Stokeslet, that is, to solve the Stokes equations where the force is not concentrated at a single point, but rather over a small ball of radius δ:

$$\mathbf{f}(\mathbf{x}) = \mathbf{f}_0\xi_\delta(\mathbf{x}-\mathbf{x}_0).$$

Here, ξ_δ is a smooth function, or blob, that satisfies $\int\xi_\delta(\mathbf{x})\,\mathrm{d}\mathbf{x} = \int\delta(\mathbf{x})\,\mathrm{d}\mathbf{x} = 1$, and is usually chosen to be radially symmetric. Also, G_δ and B_δ are then smooth approximations of G and B, and can be found by solving $\Delta G_\delta(\mathbf{x}) = \xi_\delta(\mathbf{x})$ and $\Delta B_\delta(\mathbf{x}) = G_\delta(\mathbf{x})$ in free space. Then the regularized Stokeslet is defined as the exact solution of the Stokes equations with the regularized force ([14,15])

$$p^\delta(\mathbf{x}) = \mathbf{f}_0\cdot\nabla G_\delta(\mathbf{x}-\mathbf{x}_0),$$
$$\mu\mathbf{u}^\delta(\mathbf{x}) = -\mathbf{f}_0 G_\delta(\mathbf{x}-\mathbf{x}_0) + (\mathbf{f}_0\cdot\nabla)\nabla B_\delta(\mathbf{x}-\mathbf{x}_0).$$

The linearity of the governing equations allows the superposition of solutions due to different singularities in the fluid, so for N forces $\mathbf{f}_k$ located at $\mathbf{x}_k$, we can express the pressure and velocity as

$$p^\delta(\mathbf{x}) = \sum_{k=1}^N \mathbf{f}_k\cdot\nabla G_\delta(\mathbf{x}-\mathbf{x}_k), \tag{8}$$

$$\mu\mathbf{u}^\delta(\mathbf{x}) = \mathbf{U} + \sum_{k=1}^N\{-\mathbf{f}_k G_\delta(\mathbf{x}-\mathbf{x}_k) + (\mathbf{f}_k\cdot\nabla)\nabla B_\delta(\mathbf{x}-\mathbf{x}_k)\}, \tag{9}$$

where $\mathbf{U}$ is a constant flow that can be added to make the total constant flow zero. When forces are distributed on a surface Γ described by $\mathbf{x}(s)$, the regularized Stokes solution is

$$p^\delta(\mathbf{x}) = \int_\Gamma \mathbf{f}(s)\cdot\nabla G_\delta(\mathbf{x}-\mathbf{x}(s))\mathrm{d}s,$$
$$\mu\mathbf{u}^\delta(\mathbf{x}) = \mathbf{U} + \int_\Gamma\{-\mathbf{f}(s)G_\delta(\mathbf{x}-\mathbf{x}(s)) + (\mathbf{f}(s)\cdot\nabla)\nabla B_\delta(\mathbf{x}-\mathbf{x}(s))\}\mathrm{d}s,$$

and Eqs. (8) and (9) can be viewed as a discretization of the boundary integrals by a simple quadrature.

In two dimensions, we choose the following radially symmetric blob:

$$\xi_\delta(r) = \frac{2\delta^4}{\pi(r^2+\delta^2)^3},$$

where $r = |\mathbf{x}|$. Then the corresponding regularized Green's function is

$$G_\delta(r) = \frac{1}{4\pi}\left[\ln(r^2+\delta^2) - \frac{\delta^2}{r^2+\delta^2}\right].$$

Similarly,

$$B'_\delta(r) = \frac{1}{r}\int_0^r sG_\delta(s)\,\mathrm{d}s = \frac{r}{8\pi}[\ln(r^2+\delta^2) - 1].$$

Please cite this article in press as: S. Tlupova, R. Cortez, Boundary integral solutions of coupled Stokes and Darcy flows, J. Comput. Phys. (2008), doi:10.1016/j.jcp.2008.09.011

With these, the pressure and velocity due to a single point force $\mathbf{f}_0$ are equal to

$$p^\delta(\mathbf{x}) = \frac{1}{2\pi}[\mathbf{f}_0 \cdot (\mathbf{x}-\mathbf{x}_0)]A_\delta(r_0),$$
$$\mu\mathbf{u}^\delta(\mathbf{x}) = -\frac{\mathbf{f}_0}{4\pi}H_\delta(r_0) + \frac{1}{4\pi}[\mathbf{f}_0 \cdot (\mathbf{x}-\mathbf{x}_0)](\mathbf{x}-\mathbf{x}_0)J_\delta(r_0),$$

where

$$A_\delta(r) = \frac{r^2+2\delta^2}{(r^2+\delta^2)^2}, \quad H_\delta(r) = \frac{1}{2}\ln(r^2+\delta^2) - \frac{\delta^2}{r^2+\delta^2}, \quad J_\delta(r) = \frac{1}{r^2+\delta^2}. \tag{10}$$

We can now rewrite (8) and (9) as

$$p^\delta(\mathbf{x}) = \sum_{k=1}^{N}\frac{1}{2\pi}[\mathbf{f}_k \cdot (\mathbf{x}-\mathbf{x}_k)]A_\delta(r_k),$$
$$\mathbf{u}^\delta(\mathbf{x}) = \sum_{k=1}^{N}\left\{-\frac{\mathbf{f}_k}{4\pi\mu}H_\delta(r_k) + \frac{1}{4\pi\mu}[\mathbf{f}_k \cdot (\mathbf{x}-\mathbf{x}_k)](\mathbf{x}-\mathbf{x}_k)J_\delta(r_k)\right\},$$

with $r_k = |\mathbf{x}-\mathbf{x}_k|$, which we write using vector notation as

$$\begin{pmatrix} p^\delta(\mathbf{x}) \\ \mathbf{u}^\delta(\mathbf{x}) \end{pmatrix} = \sum_{k=1}^{N}\begin{pmatrix} \mathbf{A}^p(\mathbf{x}-\mathbf{x}_k) \\ \mathbf{A}^{\mathbf{u}}(\mathbf{x}-\mathbf{x}_k) \end{pmatrix}\mathbf{f}_k, \tag{11}$$

where

$$\mathbf{A}^p(\mathbf{x}) = \frac{1}{2\pi}(xA_\delta(r), yA_\delta(r))$$

and

$$\mathbf{A}^{\mathbf{u}}(\mathbf{x}) = \frac{1}{4\pi\mu}\begin{pmatrix} -H_\delta(r)+x^2J_\delta(r) & xyJ_\delta(r) \\ xyJ_\delta(r) & -H_\delta(r)+y^2J_\delta(r) \end{pmatrix}.$$

These formulas can be used in two ways: first, if the forces on the boundary are known, they can be used to compute the fluid quantities everywhere. Second, if the forces are not known, but say, velocity is given on the boundary, the linear system that results from evaluating (11) at all boundary points can be solved for the forces and then the same formulas can be used to compute the flow anywhere. This method has been successfully applied to many problems, like swimming of helical bacteria, such as spirochetes and *E. coli* ([15,19,12]), the method of images was derived for near-wall effects ([1]), and there is still ongoing research with the use and analysis of this method.

To couple the Stokes flow with the flow in a porous medium, we find the regularized fundamental solution of Darcy's equations, i.e. we solve

$$\frac{\mu}{k}\mathbf{u}^\delta = -\nabla p^\delta + \mathbf{g}_0\xi_\delta(\mathbf{x}-\mathbf{x}_0), \quad \nabla\cdot\mathbf{u}^\delta = 0,$$

the solution to which is

$$p^\delta(\mathbf{x}) = \mathbf{g}_0 \cdot \nabla G_\delta(\mathbf{x}-\mathbf{x}_0),$$
$$\mu\mathbf{u}^\delta(\mathbf{x}) = k\{\mathbf{g}_0\xi_\delta(\mathbf{x}-\mathbf{x}_0) - (\mathbf{g}_0\cdot\nabla)\nabla G_\delta(\mathbf{x}-\mathbf{x}_0)\}.$$

The Darcy pressure has the same expression as the Stokes pressure, and the Darcy velocity is the negative Laplacian of the Stokeslet. When this solution is integrated over a boundary and a quadrature rule is applied to discretize the integrals, the resulting numerical method is

$$p^\delta(\mathbf{x}) = \sum_{j=1}^{N}\mathbf{g}_j \cdot \nabla G_\delta(\mathbf{x}-\mathbf{x}_j), \tag{12}$$

$$\mu\mathbf{u}^\delta(\mathbf{x}) = k\sum_{j=1}^{N}\{\mathbf{g}_j\xi_\delta(\mathbf{x}-\mathbf{x}_j) - (\mathbf{g}_j\cdot\nabla)\nabla G_\delta(\mathbf{x}-\mathbf{x}_j)\}, \tag{13}$$

where $\mathbf{g}_j$ approximates the total force over the patch of grid containing $\mathbf{x}_j$.

The aim of this work is to address the error made in the method and to reduce it. It is important to note that if the forces are to be computed from given velocity and pressure, the pressure equation has to be modified at the boundary, since it is known that though the velocity is continuous, the pressure integral has discontinuities across boundaries. More accurate quadrature rules could be used to discretize the boundary integrals, resulting in slight modifications of the Eq. (11), due to the weights of the specific quadrature.

Please cite this article in press as: S. Tlupova, R. Cortez, Boundary integral solutions of coupled Stokes and Darcy flows, J. Comput. Phys. (2008), doi:10.1016/j.jcp.2008.09.011

The error in the solution of (11) has two parts – the error due to regularization and the error due to the discretization of the boundary integrals, which correspond to the following dependence on the boundary discretization size h and regularization δ:

$$E(\delta, h) \approx \underbrace{C_1 \delta^t}_{\text{regularization error}} + \underbrace{C_2 \frac{h^p}{\delta^q}}_{\text{discretization error}}, \tag{14}$$

for some powers t,p,q ([15]). It can be seen from this dependence that for a fixed discretization size h, the regularization term increases with δ and dominates the error when δ is large. On the other hand, the discretization term increases without bound as $\delta \to 0$. Consequently, the error curve for fixed h has a minimum as a function of the regularization parameter δ. The value of δ that leads to this minimum error is referred to as the optimal regularization value.

2.2. A motivating example

We focus on reducing the regularization error. It was demonstrated in [15] that the regularization error is $O(\delta^2)$ in the far field and only $O(\delta)$ in the near field, i.e. when the evaluation point is close to the boundary. This is true when the forces on the boundary are known to be exact. However, we have found that when the boundary force must be computed first from velocity boundary conditions, the error in the force turns out to be $O(\delta)$ because it comes from a near-field computation. This makes the error in all subsequent computations that use the force (even in the far field) be $O(\delta)$.

We use the same test problem from [15] of a unit solid sphere centered at the origin translating with velocity $\mathbf{U} = (0,0,U_3)$, but rather than assigning the exact force density at every point on the surface, we use the boundary condition for the velocity to set up a linear system for the forces. We solve the system iteratively using GMRES and then use the resulting forces to compute the velocity at other points. The error in the boundary velocity is now only due to solving the linear system and therefore very small, but at the far-field point (1.5,0,0), the error shows only first order convergence, shown in Fig. 1. The error in velocity using the exact force density is shown in dashed. The forces computed from the linear system converge as $O(\delta)$ as well. $F3$ is the third component of the total force.

2.2.1. The idea of the correction terms

To modify the velocity formulation in the numerical method and improve the convergence of the near field to $O(\delta^2)$, consider the error due to regularization:

$$\mu\mathbf{u}(\mathbf{x}) - \mu\mathbf{u}^{\delta}(\mathbf{x}) = -\int_{\partial\Omega} \mathbf{f}(s)(G - G_\delta)(\mathbf{x} - \mathbf{x}(s))\mathrm{d}s + \int_{\partial\Omega} (\mathbf{f}(s)\cdot\nabla)\nabla(B - B_\delta)(\mathbf{x} - \mathbf{x}(s))\mathrm{d}s. \tag{15}$$

Assume $\mathbf{x}(s^*)$ is the boundary point closest to $\mathbf{x}$ (Fig. 2). If the force is smooth along the boundary, we can write $\mathbf{f}(s) = \mathbf{f}(s^*) + \mathbf{f}_s(s^*)\,(s - s^*) + O((s - s^*)^2)$ for s near s^*. For s far from s^*, the integrands are very small due to the fast decay of $G - G_\delta$. For the specific blobs discussed here,

$$G(r) - G_\delta(r) = \begin{cases} O\left(\frac{\delta^4}{r^4}\right) & \text{in } \mathbb{R}^2 \\ O\left(\frac{\delta^2}{r^3}\right) & \text{in } \mathbb{R}^3 \end{cases}$$

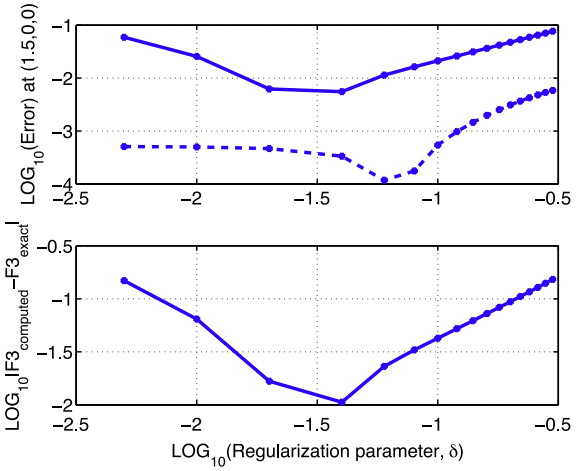

Fig. 1. $\log_{10}$ of the error in velocity at the point (1.5,0,0) with exact forces (top, dashed) and computed forces (top, solid), and $\log_{10}$ of the error in the total force (bottom).

Please cite this article in press as: S. Tlupova, R. Cortez, Boundary integral solutions of coupled Stokes and Darcy flows, J. Comput. Phys. (2008), doi:10.1016/j.jcp.2008.09.011

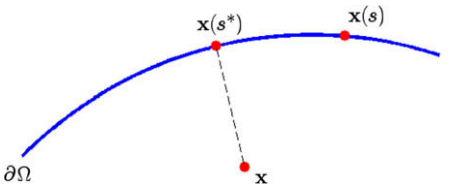

Fig. 2. Description of the boundary.

for $\delta \ll r$. This difference can be made even smaller with blobs that, for example, have compact support or decay to zero exponentially.

To increase the order of convergence, we eliminate the error due to the first term in the series expansion of the force, i.e. a new way of approximating the velocity is

$$\mu \mathbf{U}^{\delta}(\mathbf{x}) = -\int_{\partial\Omega} \mathbf{f}(s) G_{\delta}(\mathbf{x}-\mathbf{x}(s))\mathrm{d}s + \int_{\partial\Omega} (\mathbf{f}(s)\cdot\nabla)\nabla B_{\delta}(\mathbf{x}-\mathbf{x}(s))\mathrm{d}s$$
$$-\int_{\partial\Omega} \mathbf{f}(s^*)(G-G_{\delta})(\mathbf{x}-\mathbf{x}(s))\mathrm{d}s + \int_{\partial\Omega} (\mathbf{f}(s^*)\cdot\nabla)\nabla(B-B_{\delta})(\mathbf{x}-\mathbf{x}(s))\mathrm{d}s. \tag{16}$$

The first line represents the original uncorrected boundary integrals, and the second line is a correction term that reduces the regularization error to the next order of convergence. $\mathbf{f}(s^*)$ factors out of the integrals and when solving the linear system for the forces, the correction terms represent additional coefficients to the diagonal elements. The size of the matrix does not increase.

As a test example with non-constant forces, we apply a singular force $\mathbf{F} = (0,0,1)$ at the origin and compute the exact velocity on the surface of the unit sphere as a singular Stokeslet

$$\mathbf{U}(\mathbf{x}) = \frac{\mathbf{F}}{8\pi\mu} + \frac{1}{8\pi\mu}[\mathbf{F}\cdot\mathbf{x}]\mathbf{x},$$

with $|\mathbf{x}| = 1$. Now the forces on the surface of the sphere are unknown, and we set up a matrix system to compute them. We compare the original regularized formula with the corrected one. Fig. 3 shows the error in the third component of velocity as a function of the regularization size and its log–log plot for 2402 points on the surface. The regularization error is considerably reduced in magnitude and the order of convergence increases from $O(\delta)$ to $O(\delta^2)$. This indicates that adding correction terms improves convergence in the near field, and therefore, in the computed forces, to second order, so the error of the fluid velocity in the far field is $O(\delta^2)$ as well.

Next, we review some potential theory that will be used to increase accuracy when computing the two-dimensional integrals.

2.3. Potential theory

Given continuous functions ϕ and ψ on the boundary of a bounded domain $\Omega \in \mathbb{R}^2$, the integrals

$$S(\mathbf{x};\phi) = \int_{\partial\Omega} \phi(s) G(\mathbf{x}-\mathbf{x}(s))\mathrm{d}s \tag{17}$$

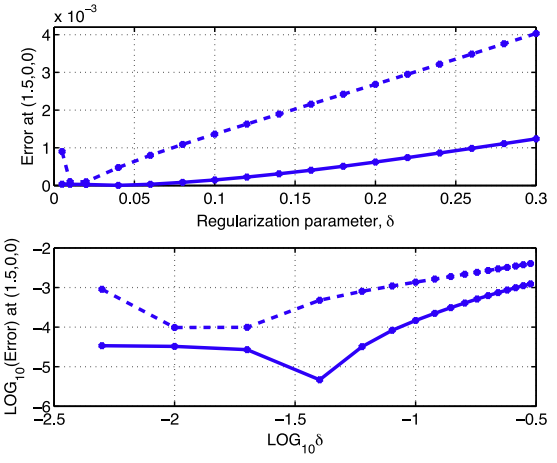

Fig. 3. Velocity error using uncorrected (dashed lines) and corrected (solid lines) expressions at the point (1.5,0,0).

Please cite this article in press as: S. Tlupova, R. Cortez, Boundary integral solutions of coupled Stokes and Darcy flows, J. Comput. Phys. (2008), doi:10.1016/j.jcp.2008.09.011

and

$$D(\mathbf{x};\psi) = \int_{\partial\Omega} \psi(s)\hat{n}(s)\cdot\nabla G(\mathbf{x}-\mathbf{x}(s))\mathrm{d}s, \tag{18}$$

are referred to as single layer and double layer potentials with densities ϕ and ψ. In the present context, the single layer potential represents the velocity potential due to a boundary distribution of point sources, whereas the double layer potential can be interpreted as the velocity potential of a boundary distribution of point-source dipoles. The classical potential theory shows that both the single and double layer potentials are harmonic functions in Ω and $\mathbb{R}^2\setminus\overline{\Omega}$ ([13,27]). In addition, for smooth boundaries, (17) is continuous across the boundary, whereas (18) has different limiting values when approaching the boundary from the interior and the exterior of the domain. These jump conditions follow from the known identity

$$\int_{\partial\Omega} \hat{n}(s)\cdot\nabla G(\mathbf{x}-\mathbf{x}(s))\mathrm{d}s = \begin{cases} -1, & \mathbf{x}\in\Omega \\ -1/2, & \mathbf{x}\in\partial\Omega \\ 0, & \mathbf{x}\in\mathbb{R}^2\setminus\overline{\Omega} \end{cases}.$$

More specifically, $D(\mathbf{x};\psi)$ has a discontinuity equal to ψ across $\partial\Omega$. Therefore, it needs some corrections in order to solve boundary value problems. For example, the solution of the Dirichlet problem

$$\Delta v = 0 \text{ in } \Omega, \quad v = g \text{ on } \partial\Omega,$$

is expressed as a double layer potential for some density ψ which is determined from g as the solution of the following Fredholm integral equation of the second kind,

$$-\frac{1}{2}\psi(\mathbf{x}) + \int_{\partial\Omega}\psi(s)\hat{n}(s)\cdot\nabla G(\mathbf{x}-\mathbf{x}(s))\mathrm{d}s = g(\mathbf{x}), \quad \mathbf{x}\in\partial\Omega.$$

Numerical treatment often involves some regularization procedure and evaluation of the integrals by a standard quadrature rule. But without special care, these integrals are nearly singular when the evaluation point is close to the boundary, since the regular kernels have large derivatives. This problem was addressed in [5,4,3]. Beale and Lai [5] developed a method for evaluating nearly singular integrals in two dimensions accurately by first regularizing the kernels and discretizing the integrals in a standard way, and then adding corrections for the low-order errors due to regularization and discretization. It was applied to Stokes equations in [14]. The method was then extended to elliptic equations in three dimensions in [4]. Motivated by this work, we rewrite all the fluid quantities in terms of potentials and calculate the first correction of the regularization error. The next step will be to compute corrections analogous to Beale and Lai's to achieve even higher accuracy.

Derivatives of potentials are also harmonic in Ω and for a boundary described by $(x(s),y(s))$, can be computed at $\mathbf{x}\in\Omega$ as ([5,35])

$$\frac{\partial}{\partial x}S(\mathbf{x};\phi) = S(\mathbf{x};(\phi x_s)_s) + D(\mathbf{x};\phi y_s), \quad \frac{\partial}{\partial x}D(\mathbf{x};\psi) = -S(\mathbf{x};(\psi_s y_s)_s) + D(\mathbf{x};\psi_s x_s),$$
$$\frac{\partial}{\partial y}S(\mathbf{x};\phi) = S(\mathbf{x};(\phi y_s)_s) - D(\mathbf{x};\phi x_s), \quad \frac{\partial}{\partial y}D(\mathbf{x};\psi) = S(\mathbf{x};(\psi_s x_s)_s) + D(\mathbf{x};\psi_s y_s).$$

3. Reformulation of the boundary integrals in R^2

The observations shown in the previous section for three dimensions will be analogous in the two-dimensional case. This means that when using the uncorrected expressions to solve boundary value problems for Stokes and Darcy flows to compute the forces, the accuracy of the solution will decrease. Note that the error is larger when we regularize more singular kernels. In this section we compute corrections of the regularization error in two dimensions for the pressure, Stokes and Darcy velocities, and velocity gradients using a slightly different approach – we first rewrite all integrals in terms of potentials.

3.1. Stokes pressure and velocity

Using the decomposition $\mathbf{f}(s) = f^{(n)}(s)\hat{n}(s) + f^{(\tau)}(s)\hat{\tau}(s)$ of the force, where $\hat{\tau}(s)$ is the tangential and $\hat{n}(s)$ is the outward normal vectors at s, the Stokes pressure and velocity at $\mathbf{x}\in\Omega$ can be written in terms of potentials as

$$p(\mathbf{x}) = \int_{\partial\Omega} f^{(n)}(s)\hat{n}(s)\cdot\nabla G(\mathbf{x}-\mathbf{x}(s))\mathrm{d}s + \int_{\partial\Omega} f_s^{(\tau)}(s)G(\mathbf{x}-\mathbf{x}(s))\mathrm{d}s = S(\mathbf{x};f_s^{(\tau)}) + D(\mathbf{x};f^{(n)}), \tag{19}$$

where the single layer potential is obtained by integration by parts, and

$$\mathbf{u}(\mathbf{x}) = \int_{\partial\Omega} -\frac{\mathbf{f}(s)}{2\mu}G(\mathbf{x}-\mathbf{x}(s))\mathrm{d}s + \int_{\partial\Omega}\frac{\mathbf{x}-\mathbf{x}(s)}{2\mu}[\mathbf{f}(s)\cdot\nabla G(\mathbf{x}-\mathbf{x}(s))]\mathrm{d}s = S(\mathbf{x};\boldsymbol{\phi}) + D(\mathbf{x};\boldsymbol{\psi}), \tag{20}$$

where

Please cite this article in press as: S. Tlupova, R. Cortez, Boundary integral solutions of coupled Stokes and Darcy flows, J. Comput. Phys. (2008), doi:10.1016/j.jcp.2008.09.011

$$\boldsymbol{\phi}(s) = -\frac{\mathbf{f}(s)}{2\mu} + \left[\frac{\mathbf{x}-\mathbf{x}(s)}{2\mu} f^{(\tau)}(s)\right]_s,$$
$$\boldsymbol{\psi}(s) = \frac{\mathbf{x}-\mathbf{x}(s)}{2\mu} f^{(n)}(s).$$

For details of derivation, refer to [14]. Note here that both the pressure and velocity have double layer parts, but the integrand is zero on the boundary for $\mathbf{u}$, whereas it is nonzero for p. This means that when $\mathbf{x} \in \partial\Omega$, the pressure has to be computed as

$$p(\mathbf{x}) = \int_{\partial\Omega} f^{(n)}(s)\hat{n}(s)\cdot\nabla G(\mathbf{x}-\mathbf{x}(s))\mathrm{d}s + \int_{\partial\Omega} f_s^{(\tau)}(s) G(\mathbf{x}-\mathbf{x}(s))\mathrm{d}s - \frac{1}{2} f^{(n)}(\mathbf{x}).$$

The numerical method with corrections is based on regularizing the functions and eliminating the highest-order error. This idea was shown in Section 2.2.1, where (15) represents the error due to regularization, and the largest part is added to the numerical solution to reduce the error, as shown in (16). Similarly, we regularize the kernels in (19) and (20) and add the leading term of regularization error to get

$$P^{\delta}(\mathbf{x}) = \int_{\partial\Omega} f^{(n)}(s)\hat{n}(s)\cdot\nabla G_{\delta}(\mathbf{x}-\mathbf{x}(s))\mathrm{d}s + \int_{\partial\Omega} f_s^{(\tau)}(s) G_{\delta}(\mathbf{x}-\mathbf{x}(s))\mathrm{d}s - f^{(n)}(s^*)\left[1 - I_{\delta}^{(n)}(\mathbf{x})\right] + f_s^{(\tau)}(s^*)\left[I^G(\mathbf{x}) - I_{\delta}^G(\mathbf{x})\right], \quad (21)$$

and

$$\mathbf{U}^{\delta}(\mathbf{x}) = \int_{\partial\Omega} \boldsymbol{\phi}(s) G_{\delta}(\mathbf{x}-\mathbf{x}(s))\mathrm{d}s + \int_{\partial\Omega} \boldsymbol{\psi}(s)\hat{n}(s)\cdot\nabla G_{\delta}(\mathbf{x}-\mathbf{x}(s))\mathrm{d}s + \boldsymbol{\phi}(s^*)[I^G(\mathbf{x}) - I_{\delta}^G(\mathbf{x})] - \boldsymbol{\psi}(s^*)[1 - I_{\delta}^{(n)}(\mathbf{x})], \quad (22)$$

for $\mathbf{x} \in \overline{\Omega}$, where we defined

$$I_{\delta}^{(n)}(\mathbf{x}) = -\int_{\partial\Omega} \hat{n}(s)\cdot\nabla G_{\delta}(\mathbf{x}-\mathbf{x}(s))\mathrm{d}s, \quad (23)$$
$$I^G(\mathbf{x}) = \int_{\partial\Omega} G(\mathbf{x}-\mathbf{x}(s))\mathrm{d}s, \quad (24)$$
$$I_{\delta}^G(\mathbf{x}) = \int_{\partial\Omega} G_{\delta}(\mathbf{x}-\mathbf{x}(s))\mathrm{d}s. \quad (25)$$

When $\mathbf{x} \in \partial\Omega$, $I_{\delta}^{(n)}(\mathbf{x}) \approx 1/2$, so the corrections take care of the double layer discontinuity automatically.

3.2. Velocity gradients

In the coupled Stokes–Darcy case, the derivatives of Stokes velocity are needed at the interface. To achieve the same accuracy everywhere, it is necessary to reformulate the integrals for the velocity gradients and compute the corrections. Since the velocity can be represented as a sum of single and double layer potentials, we can compute $\partial u/\partial y$, for example, as

$$\frac{\partial u}{\partial y}(\mathbf{x}) = \frac{\partial}{\partial y} S(\mathbf{x};\phi_1) + \frac{\partial}{\partial y} D(\mathbf{x};\psi_1) = \int_{\partial\Omega} [\phi_1(s)x'(s) - \psi_1'(s)y'(s)]\frac{\partial G(\cdot)}{\partial n(s)}\mathrm{d}s + \int_{\partial\Omega} [\phi_1(s)y'(s) + \psi_1'(s)x'(s)]' G(\cdot)\mathrm{d}s,$$

where we denote $(\cdot)' = \frac{\mathrm{d}}{\mathrm{d}s}(\cdot)$. Unlike u, $\partial u/\partial y$ has nonzero double layer integrands on $\partial\Omega$, so without modification to account for the discontinuity, the calculation will be inaccurate there.

Again, these are nearly singular integrals when $\mathbf{x}$ is near the boundary, so to gain accuracy, we compute like before, regularizing the kernels and eliminating the largest error:

$$\begin{aligned}\frac{\partial U^{\delta}}{\partial y}(\mathbf{x}) = {} & \int_{\partial\Omega} [\phi_1(s)x'(s) - \psi_1'(s)y'(s)]\frac{\partial G_{\delta}(\cdot)}{\partial n(s)}\mathrm{d}s + [\phi_1(s)x'(s) - \psi_1'(s)y'(s)]|_{s=s^*}\left[1 - I_{\delta}^{(n)}(\mathbf{x})\right] \\ & + \int_{\partial\Omega} [\phi_1(s)y'(s) + \psi_1'(s)x'(s)]' G_{\delta}(\cdot)\mathrm{d}s + [\phi_1(s)y'(s) + \psi_1'(s)x'(s)]'|_{s=s^*}[I^G(\mathbf{x}) - I_{\delta}^G(\mathbf{x})],\end{aligned}$$

which can be written as

$$\begin{aligned}\frac{\partial U^{\delta}}{\partial y}(\mathbf{x}) = {} & \int_{\partial\Omega} -\frac{f_1(s)}{2\mu}\frac{\partial G_{\delta}(\cdot)}{\partial y}\mathrm{d}s + \int_{\partial\Omega} \frac{x-x(s)}{2\mu}\left[\mathbf{f}(s)\cdot\nabla\frac{\partial G_{\delta}(\cdot)}{\partial y}\right]\mathrm{d}s + \int_{\partial\Omega} \frac{x-x(s)}{2\mu} f^{(n)}(s)\xi_{\delta}(\cdot)x'(s)\mathrm{d}s \\ & + \left\{\left[-\frac{f_1(s)}{2\mu} - \frac{x'(s)}{2\mu} f^{\tau}(s) + \frac{x-x(s)}{2\mu} f_s^{(\tau)}(s)\right]x'(s)\right\}|_{s=s^*}\left[1 - I_{\delta}^{(n)}(\mathbf{x})\right] \\ & + \left\{\left[-\frac{f_1(s)}{2\mu} - \frac{x'(s)}{2\mu} f^{\tau}(s) + \frac{x-x(s)}{2\mu} f_s^{(\tau)}(s)\right]y'(s)\right\}'|_{s=s^*}[I^G(\mathbf{x}) - I_{\delta}^G(\mathbf{x})] \\ & - \left\{\left[-\frac{x'(s)}{2\mu} f^{(n)}(s) + \frac{x-x(s)}{2\mu} f_s^{(n)}(s)\right]y'(s)\right\}|_{s=s^*}[1 - I_{\delta}^{(n)}(\mathbf{x})] \\ & + \left\{\left[-\frac{x'(s)}{2\mu} f^{(n)}(s) + \frac{x-x(s)}{2\mu} f_s^{(n)}(s)\right]x'(s)\right\}'|_{s=s^*}[I^G(\mathbf{x}) - I_{\delta}^G(\mathbf{x})]. \quad (26)\end{aligned}$$

Please cite this article in press as: S. Tlupova, R. Cortez, Boundary integral solutions of coupled Stokes and Darcy flows, J. Comput. Phys. (2008), doi:10.1016/j.jcp.2008.09.011

Details can be found in [44].

3.3. Darcy velocity

The accuracy of the numerical method in (12) and (13) is compromised due to the near singularity even more in the Darcy velocity, since the expressions are more singular. This can be seen from the fact that Darcy velocity = $-k\Delta$ Stokes velocity. To improve the accuracy, we can modify the Darcy velocity in a similar way, by using the fact that it is proportional to the pressure gradient and computing derivatives of the single and double layer potentials.

$$\begin{aligned}\mathbf{u} &= -\frac{k}{\mu}\nabla p = -\frac{k}{\mu}\nabla\left[\int_{\partial\Omega} g_s^{(\tau)}(s)G(\cdot)\mathrm{d}s + \int_{\partial\Omega} g^{(n)}(s)\hat{n}(s)\cdot\nabla G(\cdot)\mathrm{d}s\right]\\ &= -\frac{k}{\mu}\left\{-\int_{\partial\Omega} g_s^{(\tau)}(s)\hat{n}(s)\frac{\partial G(\cdot)}{\partial n(s)}\mathrm{d}s + \int_{\partial\Omega}[g_s^{(\tau)}(s)\hat{\tau}(s)]'G(\cdot)\mathrm{d}s - \int_{\partial\Omega} g_s^{(n)}(s)\hat{\tau}(s)\frac{\partial G(\cdot)}{\partial n(s)}\mathrm{d}s - \int_{\partial\Omega}[g_s^{(n)}(s)\hat{n}(s)]'G(\cdot)\mathrm{d}s\right\}.\end{aligned}$$

Once the velocity is represented in terms of the single and double layer potentials, we regularize the kernels and reduce the error like it was done for Stokes quantities in (21) and (22). Using integration by parts, it then simplifies back to ([44])

$$\begin{aligned}\mathbf{U}^{\delta}(\mathbf{x}) = -\frac{k}{\mu}\Big\{&-\int_{\partial\Omega}\mathbf{g}(s)\xi_{\delta}(\mathbf{x}-\mathbf{x}(s))\mathrm{d}s + \int_{\partial\Omega}(\mathbf{g}(s)\cdot\nabla)\nabla G_{\delta}(\mathbf{x}-\mathbf{x}(s))\mathrm{d}s + \int_{\partial\Omega} g^{(\tau)}(s)\hat{\tau}(s)\xi_{\delta}(\mathbf{x}-\mathbf{x}(s))\mathrm{d}s\\ &-[g_s^{(\tau)}(s^*)\hat{n}(s^*)+g_s^{(n)}(s^*)\hat{\tau}(s^*)][1-I_{\delta}^{(n)}(\mathbf{x})] + [g_s^{(\tau)}(s)\hat{\tau}(s)-g_s^{(n)}(s)\hat{n}(s)]'|_{s=s^*}[I^G(\mathbf{x})-I_{\delta}^G(\mathbf{x})]\Big\}.\end{aligned}$$

4. Numerical results

4.1. Two-dimensional Stokes flow with a slip boundary condition

To test the Beavers–Joseph–Saffman interface condition, consider a simplified Stokes–Darcy problem: incompressible Stokes flow in a two-dimensional rectangular region $(0,L)\times(y_a,y_b)$ driven by a uniform pressure gradient, $p(0,y)=p_0$ and $p(L,y)=p_1$. Let the lower wall be adjacent to a porous medium, but the flow there will be small enough to be neglected (see Fig. 4). The slip boundary condition here is

$$u = \frac{\sqrt{k}}{\gamma}\frac{\partial u}{\partial y}, \quad v = 0, \quad y = y_a.$$

At the upper wall, we impose the no-slip condition: $\mathbf{u}(x,y_b)=\mathbf{0}$. The exact solution in the channel is (profile shown in Fig. 4)

$$\begin{aligned}p &= \frac{p_1-p_0}{L}x + p_0,\\ \mathbf{u} &= \left(\frac{p_1-p_0}{2L\mu}(y-y^*)(y-y_b), 0\right),\end{aligned}$$

where

$$y^* = y_a - \frac{\frac{\sqrt{k}}{\gamma}(y_b-y_a)}{\frac{\sqrt{k}}{\gamma}+y_b-y_a}.$$

The numerical experiments were performed with the non-dimensional parameter values $\mu=1$, $L=1$, $y_a=0.3$, $y_b=0.6$, $p_0=2.5$, $p_1=0.5$, $k=2\cdot10^{-6}$, $\gamma=0.1$. We compare two solutions, the first one obtained by approximating the original regularized boundary integrals by the trapezoidal quadrature,

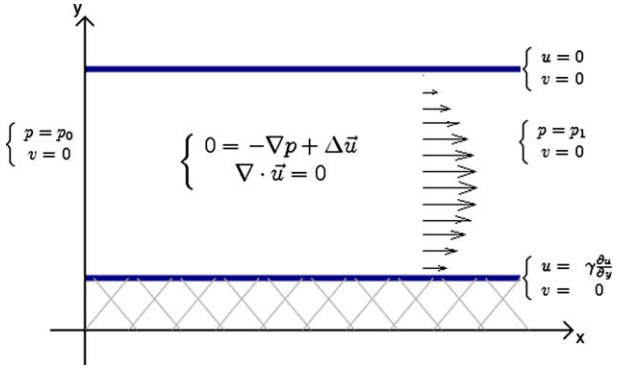

Fig. 4. Setup of the slip problem.

$$p^{\delta}(\mathbf{x}) = \sum_k \frac{1}{2\pi}[\mathbf{f}_k \cdot (\mathbf{x}-\mathbf{x}_k)]A_\delta(r_k)\Delta s_k - \chi(\mathbf{x})\frac{1}{2}f^{(n)}(s^*),$$

$$\mathbf{u}^{\delta}(\mathbf{x}) = \sum_k \left\{ -\frac{\mathbf{f}_k}{4\pi\mu}H_\delta(r_k) + \frac{1}{4\pi\mu}[\mathbf{f}_k \cdot (\mathbf{x}-\mathbf{x}_k)](\mathbf{x}-\mathbf{x}_k)J_\delta(r_k)\right\}\Delta s_k,$$

where s is the parametrization of the boundary, $\mathbf{x}(s^*)$ is the boundary point closest to $\mathbf{x}$, $A_\delta(r)$, $H_\delta(r)$, $J_\delta(r)$ are defined in (10), $\chi(\mathbf{x})$ is 1 if $\mathbf{x}$ is on the boundary ($\mathbf{x} = \mathbf{x}(s^*)$) and 0 otherwise. The second solution is obtained by the same discretization of the corrected Eqs. (21) and (22),

$$P^{\delta}(\mathbf{x}) = \sum_k \frac{1}{2\pi}[\mathbf{f}_k \cdot (\mathbf{x}-\mathbf{x}_k)]A_\delta(r_k)\Delta s_k - f^{(n)}(s^*)[1-I_\delta^{(n)}(\mathbf{x})] + f_s^{(\tau)}(s^*)[I^G(\mathbf{x}) - I_\delta^G(\mathbf{x})],$$

$$\begin{aligned}\mathbf{U}^{\delta}(\mathbf{x}) = {} & \sum_k \left\{ -\frac{\mathbf{f}_k}{4\pi\mu}\left[H_\delta(r_k) + \frac{\delta^2}{2}J_\delta(r_k)\right] + \frac{1}{4\pi\mu}[\mathbf{f}_k \cdot (\mathbf{x}-\mathbf{x}_k)](\mathbf{x}-\mathbf{x}_k)A_\delta(r_k)\right\}\Delta s_k \\ & + \left[-\frac{\mathbf{f}(s^*)}{2\mu} - \frac{\mathbf{x}'(s^*)}{2\mu}f^{(\tau)}(s^*) + \frac{\mathbf{x}-\mathbf{x}(s^*)}{2\mu}f_s^{(\tau)}(s^*)\right]\left[I^G(\mathbf{x}) - I_\delta^G(\mathbf{x})\right] - \frac{\mathbf{x}-\mathbf{x}(s^*)}{2\mu}f^{(n)}(s^*)[1-I_\delta^{(n)}(\mathbf{x})],\end{aligned}$$

where I^G, I_δ^G, and $I_\delta^{(n)}$ are given in (23)–(25).

In both uncorrected and corrected cases, we first set up the matrix system for the unknown forces $\mathbf{f}_k$ on the boundary with the boundary conditions on the right hand side. Derivatives of f are computed using second-order finite differences. We solve the linear system and once the forces are known, we compute the flow all throughout the channel.

Fig. 5 shows the profiles at $x = L/2$ of the exact velocity and velocity computed using the uncorrected expressions. We use a grid size $\Delta s = 1/80$, and a regularization parameter $\delta = \Delta s$.

The fault of straightforward differentiation of the regularized Stokeslet is apparent in this example. Since we are not using corrections here, the velocity on the lower boundary is not computed correctly. The reason is that the boundary condition on the lower boundary involves $\partial u/\partial y$, and the derivative of a single-layer potential involves a double-layer potential, therefore, needs to be modified at the boundary to represent a continuous function. So when computing the gradient of the velocity (or stresses), one has to consider that although the Stokeslet is continuous, its derivative will have a double-layer potential and without modifications will be discontinuous at the boundary. In this case, using the modified expressions is essential. The formula for $\partial U^{\delta}/\partial y$ is given in (26), which for our blob gives the following discretized equation:

$$\begin{aligned}\frac{\partial U^{\delta}}{\partial y}(\mathbf{x}) = {} & \sum_k -\frac{f_k^1}{4\pi\mu}\left[\frac{r_k^2+2\delta^2}{(r_k^2+\delta^2)^2}\right](y-y_k)\Delta s_k + \sum_k \frac{f_k^2}{4\pi\mu}\left[\frac{r_k^2+2\delta^2}{(r_k^2+\delta^2)^2}\right](x-x_k)\Delta s_k \\ & + \sum_k -\frac{1}{2\pi\mu}[f_k^1(x-x_k) + f_k^2(y-y_k)]\left[\frac{r_k^2+3\delta^2}{(r_k^2+\delta^2)^3}\right](x-x_k)(y-y_k)\Delta s_k + \sum_k \frac{f_k^{(n)}}{2\pi\mu}x_k'\left[\frac{2\delta^4}{(r_k^2+\delta^2)^3}\right](x-x_k)\Delta s_k \\ & + \left[-\frac{f_1(s^*)}{\mu} + \frac{x-x(s^*)}{2\mu}f_s^{(\tau)}(s^*)\right][1-I_\delta^{(n)}(\mathbf{x})] + \left[-\frac{f_s^{(n)}(s^*)}{\mu} + \frac{x-x(s^*)}{2\mu}f_{ss}^{(n)}(s^*)\right][I^G(\mathbf{x}) - I_\delta^G(\mathbf{x})],\end{aligned}$$

where on the lower boundary of the channel, $y = y_a$, we assume that $x'(s) = 1$, $y'(s) = 0$, $f^{(n)}(s) = -f_2(s)$, $f^{(\tau)}(s) = f_1(s)$.

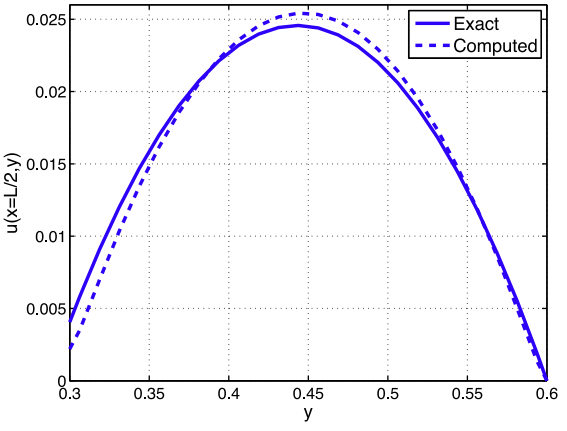

Fig. 5. Velocity profile in the middle cross-section of the channel.

Please cite this article in press as: S. Tlupova, R. Cortez, Boundary integral solutions of coupled Stokes and Darcy flows, J. Comput. Phys. (2008), doi:10.1016/j.jcp.2008.09.011

Notice that in the uncorrected case the slip velocity in Fig. 5 on the bottom boundary is about half of what it is supposed to be (which is due to the jump the double layer part of $\partial u/\partial y$ has across the boundary). The pressure also suffers from the same problem.

To investigate the dependence of the regularization error on the regularization size δ, we used a fixed discretization size of $\Delta s = 1/80$ and varied δ. Fig. 6 shows the ∞-norm errors in velocity and pressure, computed using vector norms as

two-norm velocity error = $\{\sum \Delta s[(u_{\text{exact}} - u_{\text{computed}})^2 + (v_{\text{exact}} - v_{\text{computed}})^2]\}^{1/2}$,
∞-norm velocity error = $\max(|u_{\text{exact}} - u_{\text{computed}}| + |v_{\text{exact}} - v_{\text{computed}}|)$,
two-norm pressure error = $\{\sum \Delta s[(p_{\text{exact}} - p_{\text{computed}})^2]\}^{1/2}$,
∞-norm pressure error = $\max(|p_{\text{exact}} - p_{\text{computed}}|)$.

The two-norm errors behave the same. Notice that both the velocity and pressure errors reach 5–10% in the uncorrected case, and are considerably reduced by a factor of 10 or more in the corrected case. The advance from first order convergence to second is apparent.

Fig. 7 shows graphs of velocities at $x = L/2$, computed with $\delta = \Delta s$ and $\delta = 3\Delta s$, and the corresponding pressures at $y = (y_a + y_b)/2$. The corrected velocity and pressure with $\delta = \Delta s$ practically overlap the exact solution.

4.2. Darcy flow in two dimensions

For better interpretation of the coupled test examples, we wish to investigate the effect regularization and the quadrature have on the solution of Darcy flow, as this type or regularization has not been applied to porous media flow. The kernels are now more singular, and to ensure smoothness of solutions we will use a cubic spline parametrization of the boundary, i.e. it will be a collection of cubic polynomials

$$\mathbf{x} = (x, y) = \mathbf{a}_i + \mathbf{b}_i(\alpha - \alpha_i) + \mathbf{c}_i(\alpha - \alpha_i)^2 + \mathbf{d}_i(\alpha - \alpha_i)^3,$$

for $\alpha_i \leqslant \alpha \leqslant \alpha_{i+1}$, $i = 1, \ldots, N$, with periodic boundary conditions. The arclength $s = s(\alpha)$ is a smooth map with $ds/d\alpha = |d\mathbf{x}/d\alpha|$, and the unit tangent and normal vectors are $\hat{\tau}(\alpha) = T(\alpha)/|T(\alpha)|$, $\hat{n}(\alpha) = N(\alpha)/|N(\alpha)|$, where $T(\alpha) = (x'(\alpha), y'(\alpha)) = \mathbf{b}$ and $N(\alpha) = (y'(\alpha), -x'(\alpha)) = \mathbf{b}^{\perp}$. We also have

$$\hat{\tau}_s(\alpha) = T'(\alpha)/|T(\alpha)|^2 - T(\alpha)[T(\alpha) \cdot T'(\alpha)]/|T(\alpha)|^4 = 2\mathbf{c}/|\mathbf{b}|^2 - \mathbf{b}[2\mathbf{b} \cdot \mathbf{c}]/|\mathbf{b}|^4.$$

With this parametrization, we rewrite the integrals with respect to α.

We consider two-dimensional Darcy flow with velocity given on the boundary of $\Omega = \{(x, y): x^2 + y^2 \leqslant 1\}$. This problem has a smooth boundary parametrized by $x = \cos(\alpha)$, $y = \sin(\alpha)$ for $0 \leqslant \alpha \leqslant 2\pi$. As a simple test case, consider the following exact solution

$$\mathbf{u} = ((2x - 1)(y - 1), x(x - 1) - (y - 1)^2),$$
$$p = \frac{\mu}{k}\left[x(1 - x)(y - 1) + \frac{(y - 1)^3}{3} + \frac{1}{3}\right].$$

Parameter values used are $\mu = 1$, $k = 1$.

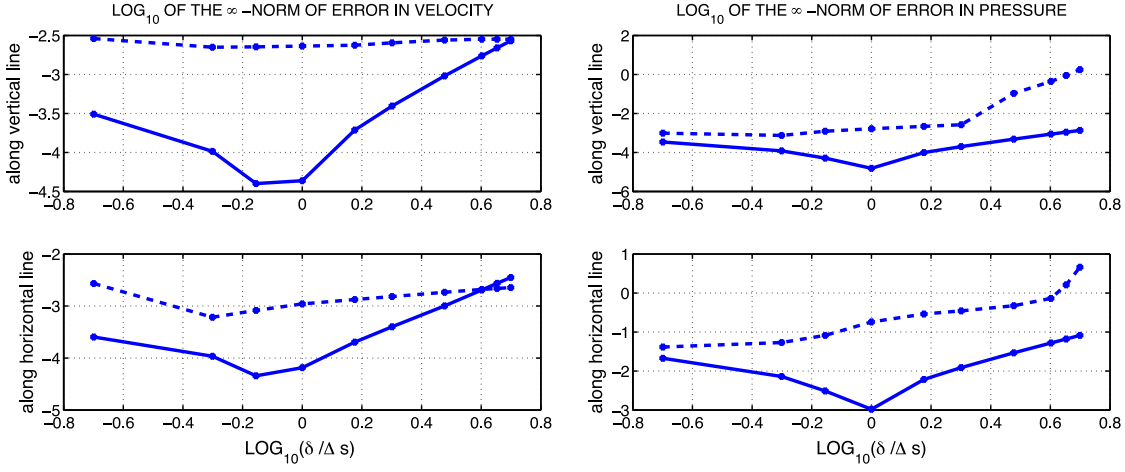

Fig. 6. Log_{10} of the ∞-norm error in velocity (left) and pressure (right) at points along the lines $x = L/2$ and $y = (y_a + y_b)/2$ (dashed – uncorrected solution, solid – corrected).

Please cite this article in press as: S. Tlupova, R. Cortez, Boundary integral solutions of coupled Stokes and Darcy flows, J. Comput. Phys. (2008), doi:10.1016/j.jcp.2008.09.011

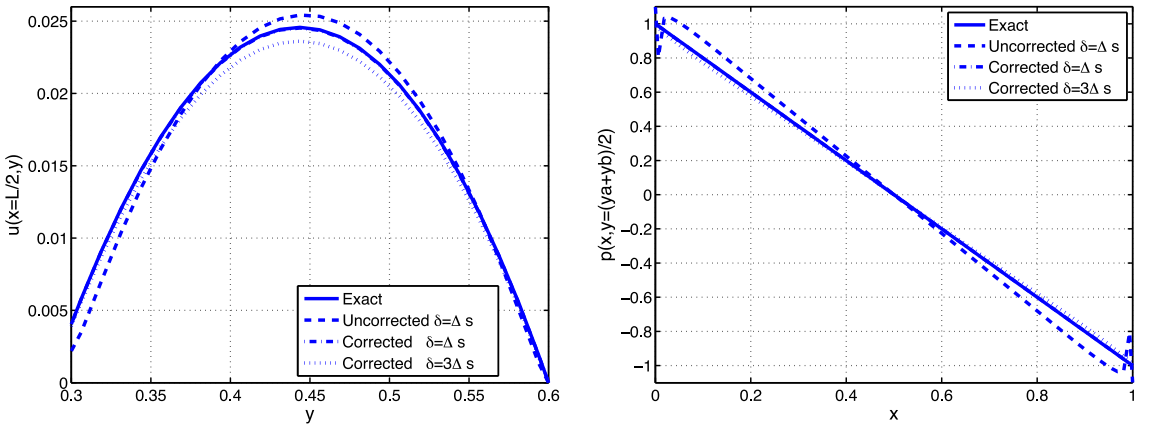

Fig. 7. Velocity u profiles in the middle cross-section of the channel (left) and pressure along the centerline of the channel (right).

To investigate the velocity expressions, we solve the full Darcy's equations on the unit disc with velocity boundary conditions. The uncorrected velocity is computed as

$$\mathbf{u}^{\delta}(\mathbf{x}) = \frac{k}{2\pi\mu}\sum_k \{\mathbf{g}_k Q_\delta(r_k) + [\mathbf{g}_k\cdot(\mathbf{x}-\mathbf{x}_k)](\mathbf{x}-\mathbf{x}_k)R_\delta(r_k)\}\Delta s_k,$$

where

$$Q_\delta(r) = \frac{4\delta^4}{(r^2+\delta^2)^3} - \frac{r^2+2\delta^2}{(r^2+\delta^2)^2},$$
$$R_\delta(r) = \frac{2(r^2+3\delta^2)}{(r^2+\delta^2)^3}.$$

The corrected velocity, on the other hand, is discretized as

$$\mathbf{U}^{\delta}(\mathbf{x}) = \frac{k}{2\pi\mu}\sum_k \{\mathbf{g}_k Q_\delta(r_k) + [\mathbf{g}_k\cdot(\mathbf{x}-\mathbf{x}_k)](\mathbf{x}-\mathbf{x}_k)R_\delta(r_k)\}\Delta s_k - \frac{k}{\mu}\sum_k g_k^{(\tau)}\hat{\tau}(s_k)\xi_\delta(r_k)\Delta s_k - \frac{k}{\mu}\mathbf{W}^*,$$

where $\Delta s = \frac{\mathrm{d}s}{\mathrm{d}\alpha}\Delta\alpha$ and

$$\mathbf{W}^* = (W^*, Z^*) = -[g_s^{(\tau)}(s^*)\hat{n}(s^*) + g_s^{(n)}(s^*)\hat{\tau}(s^*)][1 - I_\delta^{(n)}(\mathbf{x})] + [g_s^{(\tau)}(s)\hat{\tau}(s) - g_s^{(n)}(s)\hat{n}(s)]'|_{s=s^*}[I^G(\mathbf{x}) - I_\delta^G(\mathbf{x})].$$

Suppose the tangent and normal components of the forces on the boundary are cubic splines as well, i.e.

$$g^\tau(\alpha) = a_i^\tau + b_i^\tau(\alpha-\alpha_i) + qc_i^\tau(\alpha-\alpha_i)^2 + d_i^\tau(\alpha-\alpha_i)^3,$$
$$g^n(\alpha) = a_i^n + b_i^n(\alpha-\alpha_i) + c_i^n(\alpha-\alpha_i)^2 + d_i^n(\alpha-\alpha_i)^3,$$

for $\alpha_i \leqslant \alpha \leqslant \alpha_{i+1}$. The number of unknowns is reduced by the periodic spline conditions. As before, $\frac{\mathrm{d}(\cdot)}{\mathrm{d}s} = \frac{\mathrm{d}(\cdot)}{\mathrm{d}\alpha}/|\frac{\mathrm{d}\mathbf{x}}{\mathrm{d}\alpha}|$.

With this representation, higher-order integration techniques can be used without increasing the size of the linear system. Here we will compare results obtained using the trapezoidal rule and the four-point Gaussian quadrature.

We present results for $N = 200$ points and $\Delta\alpha = 2\pi/N$. Fig. 8 shows graphs of errors in velocity at $x = 0$, computed with $\delta = 3\Delta s$, and the corresponding pressure at $y = 0$. Notice that in the uncorrected case the velocity has errors of more than 20% near the boundaries, and the pressure shows even larger errors of 70%. The corrected velocity and pressure with $\delta = 3\Delta s$ eliminate the leading error term and practically overlap the exact solution.

Fig. 9 shows the two-norm errors in the first velocity component u and pressure. The first corrections reduce the regularization error in magnitude by factors of 100 and more, and increase the order of convergence. Fig. 10 shows the log–log graph of ∞-norm error in the normal component of the force, F^n. The exact normal force is equal to the jump in pressure across the boundary.

The advantage of using a higher-order integration method like Gaussian quadrature is apparent in Figs. 9 and 10. As discussed earlier in (14), for the larger values of δ, the quadrature error is overwhelmed by the regularization error and we observe no difference using either quadrature. However, as δ decreases, the optimal regularization value depends on all terms in the error expression. A more accurate quadrature (e.g. Gaussian) leads to smaller optimal regularization value and smaller minimum error.

We can analyze the dependence of the total numerical error on the discretization size h. To do this, we compute the power p in (14) as

Please cite this article in press as: S. Tlupova, R. Cortez, Boundary integral solutions of coupled Stokes and Darcy flows, J. Comput. Phys. (2008), doi:10.1016/j.jcp.2008.09.011

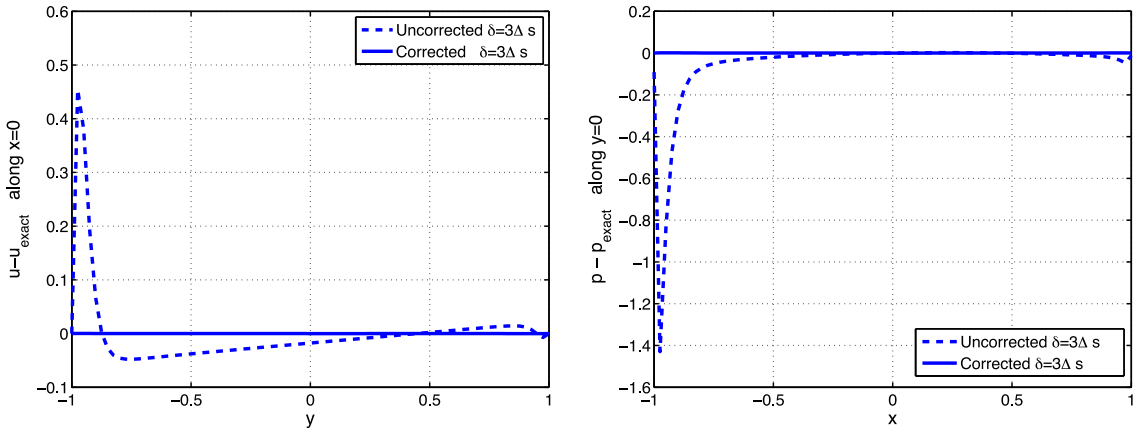

Fig. 8. Error in velocity u along the line $x = 0$ (left) and pressure along the line $y = 0$ (right).

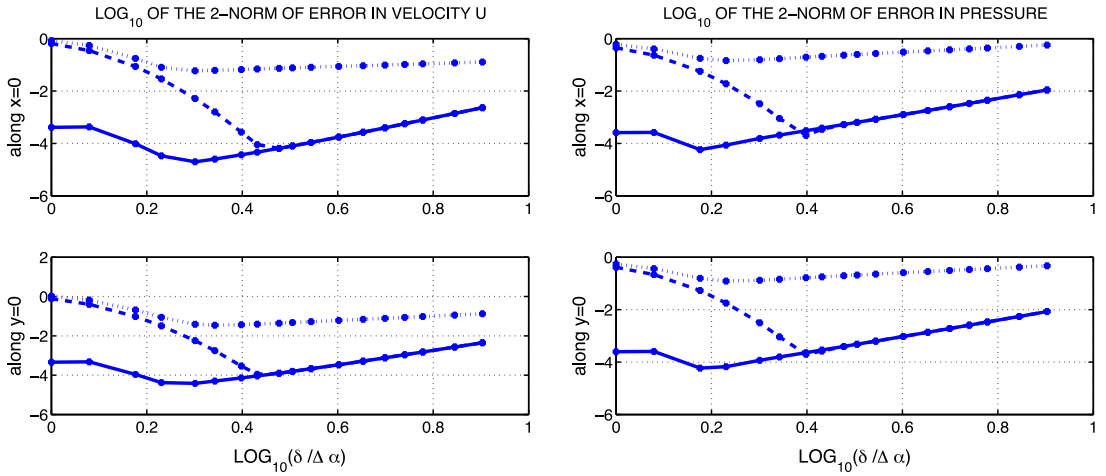

Fig. 9. Log_{10} of the two-norm error in velocity u (left) and pressure p (right) at points along different lines (dotted – uncorrected solution, dashed – corrected using trapezoidal rule, solid – corrected using Gaussian quadrature).

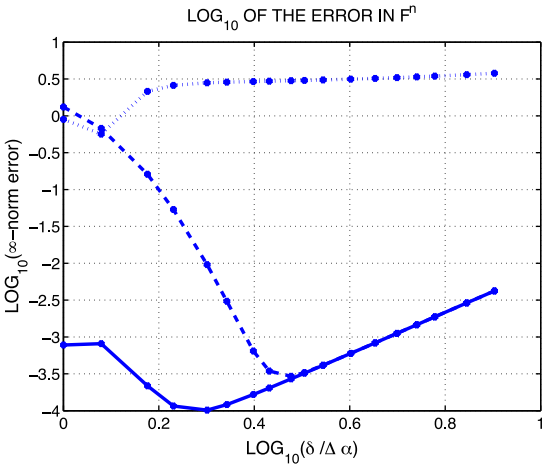

Fig. 10. Log_{10} of the ∞-norm error in the normal component of force F^n on the boundary (dotted – uncorrected solution, dashed – corrected using trapezoidal rule, solid – corrected using Gaussian quadrature).

Please cite this article in press as: S. Tlupova, R. Cortez, Boundary integral solutions of coupled Stokes and Darcy flows, J. Comput. Phys. (2008), doi:10.1016/j.jcp.2008.09.011

Table 1
The ∞-norm errors in the normal component of the force F^n computed using trapezoidal and Gaussian quadratures with h and $h/2$, with $h = 2\pi/200$, and powers of h

δ/h	Err_h TR	$\mathrm{Err}_{h/2}$ TR	Pow(h)	Err_h GQ	$\mathrm{Err}_{h/2}$ GQ	Pow(h)
1.0	1.3174	1.9018e−02	6.11	7.7696e−04	3.0783e−05	4.66
1.5	0.16138	8.2174e−05	10.94	2.1723e−04	3.4574e−05	2.65
1.7	0.05364	5.3064e−05	9.98	1.1545e−04	4.8883e−05	1.24
2.0	9.5905e−03	7.7330e−05	6.95	1.0175e−04	7.7267e−05	0.40
2.2	3.0517e−03	1.0139e−04	4.91	1.2095e−04	1.0130e−04	0.26
2.5	6.4434e−04	1.4607e−04	2.14	1.6558e−04	1.4598e−04	0.18
3.0	2.9305e−04	2.4683e−04	0.25	2.6970e−04	2.4699e−04	0.13
3.5	4.1324e−04	3.8526e−04	0.10	4.1194e−04	3.8532e−04	0.10
4.0	5.9743e−04	5.6690e−04	0.08	5.9734e−04	5.6692e−04	0.08

$$p = \frac{\log_{10}(E(h,\delta)) - \log_{10}(E(h/2,\delta))}{\log_{10} 2}.$$

The results for F^n using trapezoidal rule (TR) and Gaussian quadrature (GQ) are shown in Table 1. All computations are performed using corrections. The ∞-norm errors are shown for $N = 200$ and $N = 400$ points, i.e. h and $h/2$, where $h = 2\pi/200$. The order p is shown as pow(h). For the smallest values of δ (top three rows), the discretization error is relatively large compared to the regularization error, so we may assume that the total error is dominated by the discretization error. By looking across one of these rows, we see that the error decreases dramatically when h is reduced by a factor of two. This large rate of convergence is due to the high accuracy of the quadratures on a circle. We also notice that the Gaussian quadrature generally yields smaller errors than the trapezoid rule. As δ increases (rows four and above), the regularization error becomes dominant and the rows show that decreasing h no longer has any effect since the total error is essentially all due to the regularization. This is supported by the fact that the values in columns three and six of the table (rows four and above) are nearly identical for the two quadrature rules. The fastest convergence will be achieved by decreasing h and δ while keeping the ratio δ/h near the optimal value – in this case, $\delta/h \approx 3.0$ for TR and $\delta/h \approx 2.0$ for GQ.

4.3. Coupled problems

Next we present examples where Stokes flow is coupled to Darcy through the interface conditions. This is done by using the integral representation of Stokes quantities with boundary forces **f**, and Darcy quantities with the corresponding boundary forces **g**. Imposing all conditions at once results in a matrix system to be solved for **f** and **g** simultaneously. Once the forces are known, either flow can be computed using the corresponding force distribution.

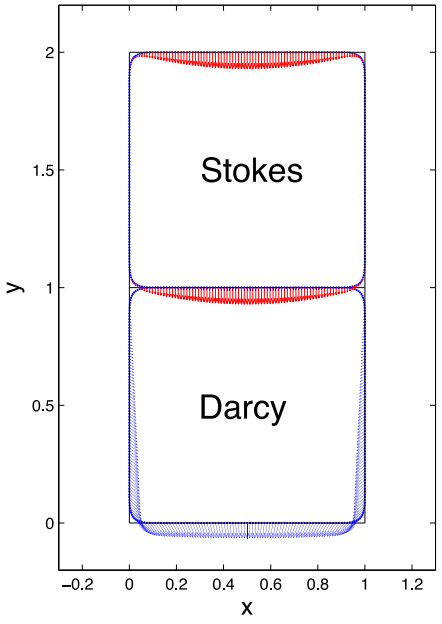

Fig. 11. Setup for coupled problem. Arrows show velocities along the boundary.

Please cite this article in press as: S. Tlupova, R. Cortez, Boundary integral solutions of coupled Stokes and Darcy flows, J. Comput. Phys. (2008), doi:10.1016/j.jcp.2008.09.011

4.3.1. Zero tangential velocity along the interface

Consider Darcy flow in $0 \leqslant x \leqslant 1$, $0 \leqslant y \leqslant 1$ and Stokes flow in $0 \leqslant x \leqslant 1$, $1 \leqslant y \leqslant 2$ with the exact solution

$$p_D = \frac{\mu}{k}\left[x(1-x)(y-1) + \frac{(y-1)^3}{3}\right] + 2\mu,$$

$$\mathbf{u}_D = \left((2x-1)(y-1), x(x-1) - (y-1)^2\right),$$

$$p_S = 2\mu y,$$

$$\mathbf{u}_S = (0, x(x-1)).$$

This solution satisfies continuity of normal components of velocity and normal force and the Beavers–Joseph–Saffman condition along the interface $y = 1$. We prescribe the velocity on the other boundaries and smooth out the corners for regularity of the boundary (see Fig. 11).

Referring to Fig. 11, the Stokeslet force field $\mathbf{f}(s)$ is defined all around the Stokes domain while the Darcy force field $\mathbf{g}(s)$ is defined on the boundary of the Darcy domain. Each boundary is represented by cubic splines through $N = 328$ nodes, so that the distance between adjacent nodes is $\Delta\alpha = 0.0122$. The force fields in the corresponding domains are also represented by cubic splines and the node values are the unknowns to be solved for. Note that both force fields exist at the common interface. Parameters $\mu = 1$, $k = 1$, $\gamma = 100$ were used and $\delta = 3\Delta\alpha$ and $\delta = \Delta\alpha$ were taken for Darcy and Stokes respectively. Figs. 12 and 13 show errors in Darcy and Stokes velocities in each domain (notice the scale difference between corrected and uncorrected figures). Two-norms of these errors at points along the centerlines for different values of δ are given in Figs. 14 and 15. GMRES tolerances were taken as 10^{-4} for uncorrected and 10^{-6} for corrected solutions due to the convergence time constraints imposed by the matrix condition numbers. When the errors are above the tolerance, it can be seen that using corrections gives smaller errors and faster convergence.

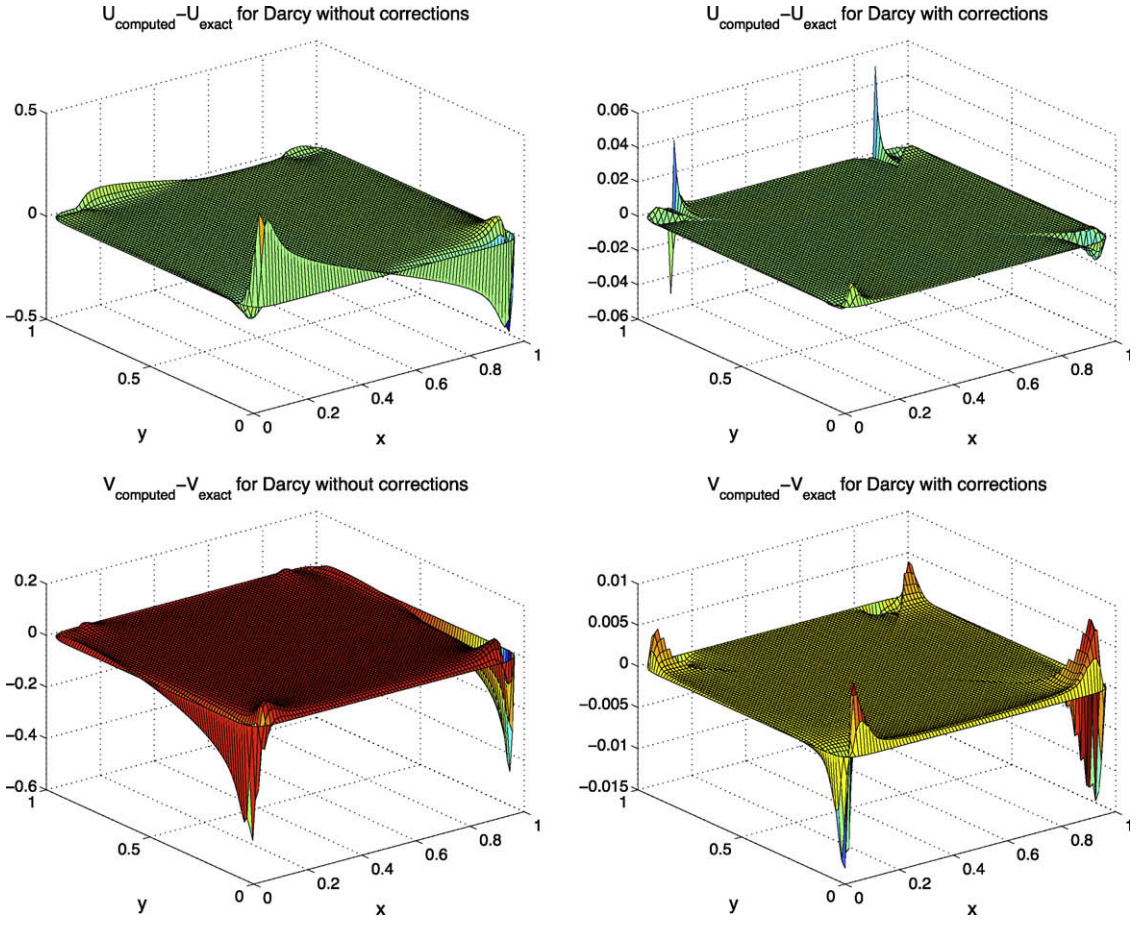

Fig. 12. Error in Darcy velocities without (left) and with (right) corrections.

Please cite this article in press as: S. Tlupova, R. Cortez, Boundary integral solutions of coupled Stokes and Darcy flows, J. Comput. Phys. (2008), doi:10.1016/j.jcp.2008.09.011

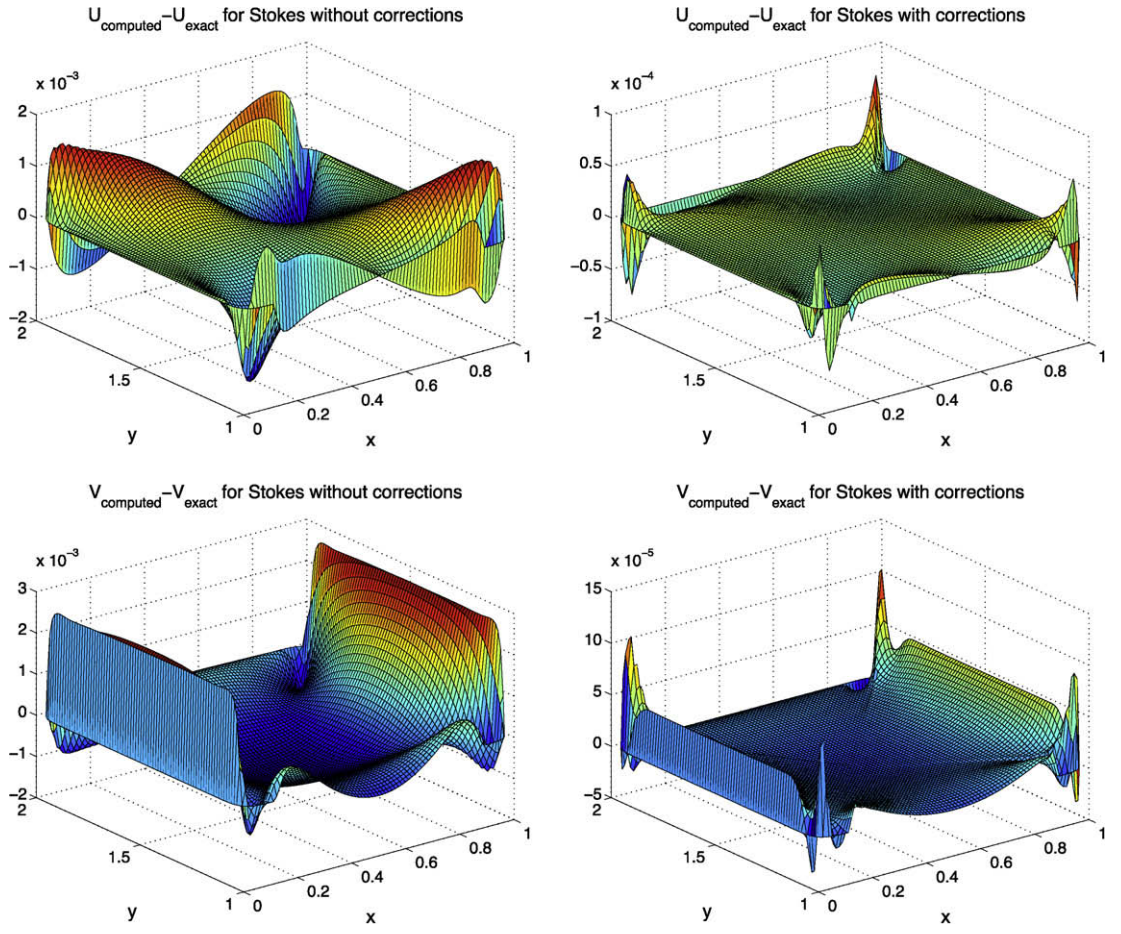

Fig. 13. Error in Stokes velocities without (left) and with (right) corrections.

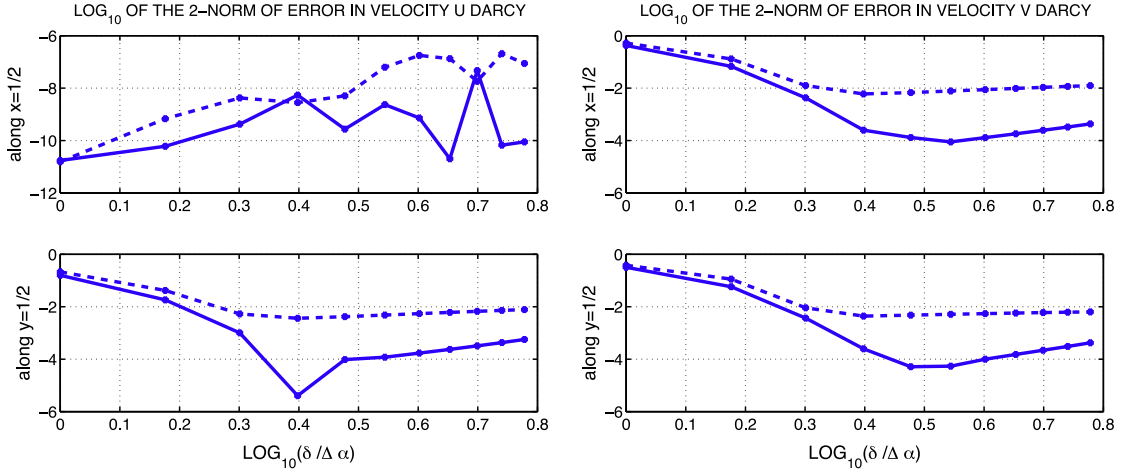

Fig. 14. Coupled solution: two-norm error in Darcy velocities u (left) and v (right) along different lines (dashed – uncorrected, solid – corrected).

4.3.2. Non-zero tangential velocity along the interface

Consider the coupled problem with a slightly modified exact solution

$$p_D = \frac{\mu}{k}\left[x(1-x)(y-1) + \frac{(y-1)^3}{3}\right] + 2\mu x,$$

Please cite this article in press as: S. Tlupova, R. Cortez, Boundary integral solutions of coupled Stokes and Darcy flows, J. Comput. Phys. (2008), doi:10.1016/j.jcp.2008.09.011

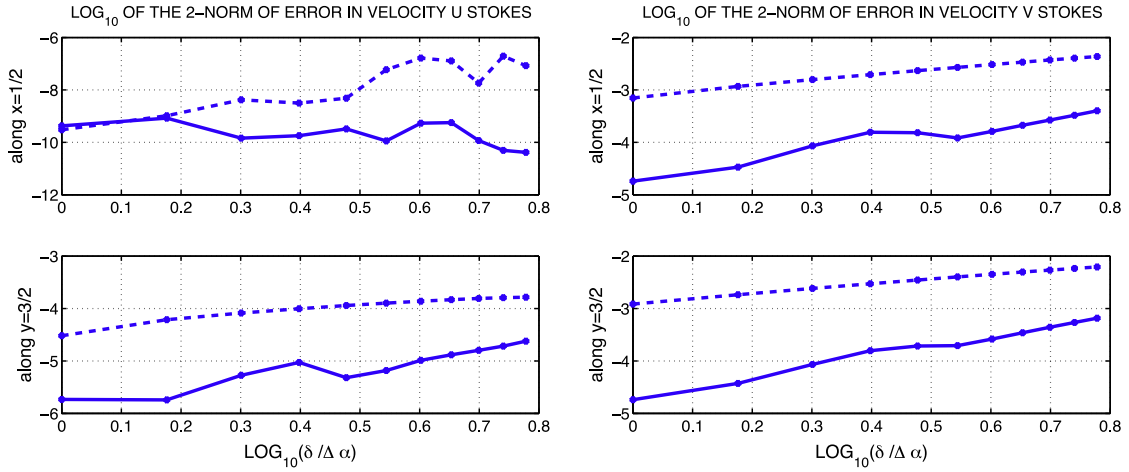

Fig. 15. Coupled solution: two-norm error in Stokes velocities u (left) and v (right) along different lines (dashed – uncorrected, solid – corrected).

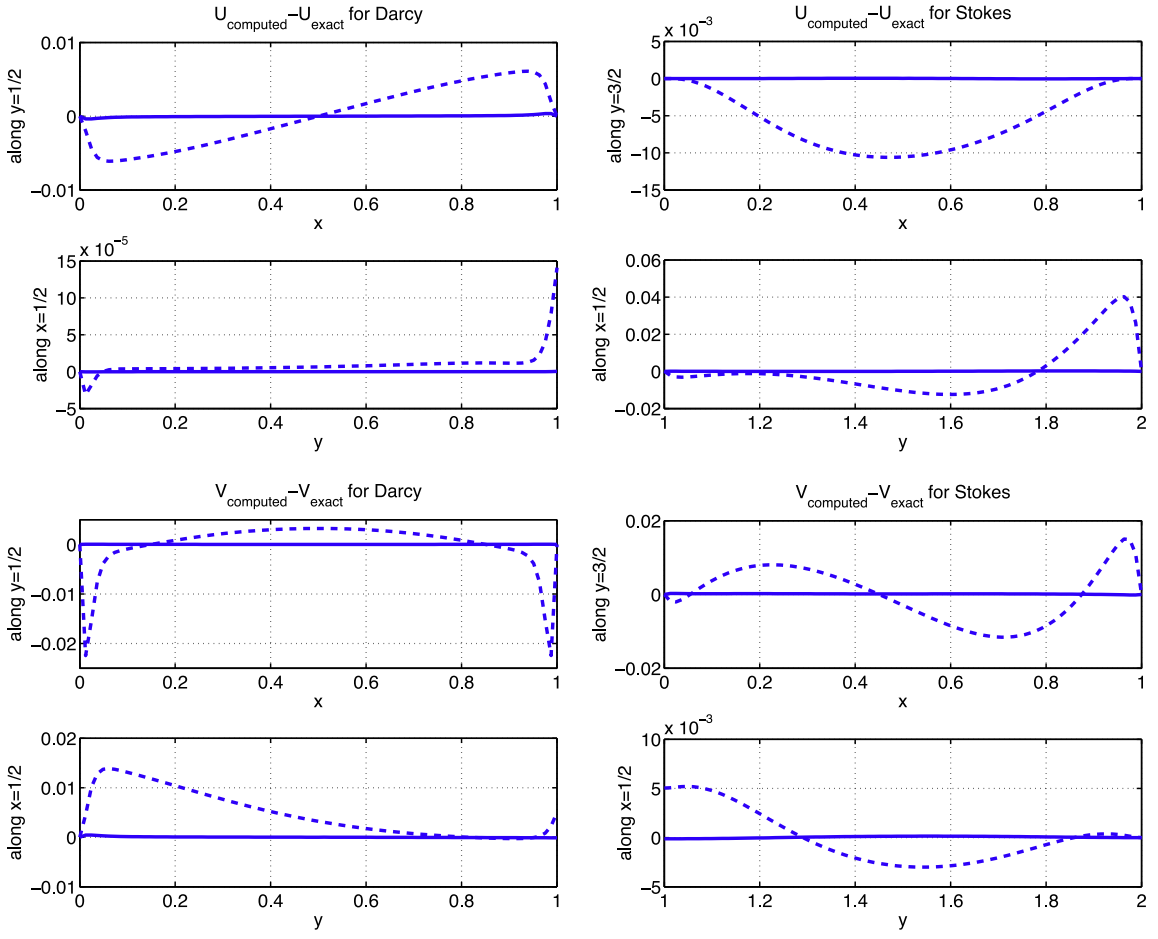

Fig. 16. Error in Darcy and Stokes velocities along different lines (dashed – uncorrected, solid – corrected).

$$\mathbf{u}_D = ((2x-1)(y-1) - 2k, x(x-1) - (y-1)^2),$$
$$p_S = 2\mu(x+y-1),$$
$$\mathbf{u}_S = \left((y-1)^2 + (y-1) + \frac{\sqrt{k}}{\gamma}, x(x-1)\right).$$

Please cite this article in press as: S. Tlupova, R. Cortez, Boundary integral solutions of coupled Stokes and Darcy flows, J. Comput. Phys. (2008), doi:10.1016/j.jcp.2008.09.011

This solution now has a non-zero tangential velocity along the interface $y = 1$, and it should be determined from the Beavers–Joseph–Saffman condition.

Fig. 16 shows errors in Darcy and Stokes velocities along the centerlines of each domain. Parameters $\mu = 1$, $k = 10^{-4}$, $\gamma = 10$ were used and $\delta = 3\Delta\alpha$ was taken for both solutions, where for $N = 328$ points on each boundary Darcy and Stokes we have $\Delta\alpha = 0.0122$.

The corrected errors are almost indistinguishable from zero compared to the uncorrected errors (they are about 1–2 orders smaller which can be seen from the following graphs). Also, from the graphs of error in v it can be seen that the continuity condition at $y = 1$ gives a much better agreement with the exact solution in the corrected case.

Note that along the interface $y = 1$, the Beavers–Joseph–Saffman condition gives $u_S = \frac{\sqrt{k}}{\gamma}\frac{\partial u_S}{\partial y} = \sqrt{k}/\gamma = 10^{-3}$, and the numerical error in the graphs is $U_S^\delta - u_S = 6.2 \times 10^{-5}$ and $U_S^\delta - u_S = 5.8 \times 10^{-7}$ at $(x,y) = (1/2, 1)$ in the uncorrected and corrected cases, respectively. u is the exact velocity and U^δ is the computed solution. The exact Darcy velocity along the interface is $u_D = -2k = -2 \times 10^{-4}$, and we get errors $U_D^\delta - u_D = 1.4 \times 10^{-4}$ with uncorrected and $U_D^\delta - u_D = -1.7 \times 10^{-7}$ with corrected solutions. The Darcy error in the uncorrected case is of the same order as both the exact solution and the GMRES tolerance which is the smallest for the iterations to converge. With the corrected solution, we get better conditioned systems that converge faster and give more accurate solutions.

4.3.3. Discontinuous pressure along the interface

Next, we modify the exact solution so that the pressure is not continuous across the interface,

$$p_D = \frac{\mu}{k}\left[x(1-x)(y-1) + \frac{(y-1)^3}{3}\right] + 2\mu x + 2\mu\frac{\sqrt{k}}{\gamma},$$
$$\mathbf{u}_D = ((2x-1)(y-1) - 2k, x(x-1) - (y-1)^2),$$
$$p_S = \mu(2x + y - 1),$$
$$\mathbf{u}_S = \left((y-1)^2 + x(y-1) + x\frac{\sqrt{k}}{\gamma}, x(x-1) - \frac{(y-1)^2}{2} - \frac{\sqrt{k}}{\gamma}(y-1)\right).$$

The interface conditions are imposed as before. For the continuity of normal forces, the stress tensor needs to be computed for Stokes flow. To obtain the uncorrected expressions, the regularized Stokeslet is simply differentiated in x and y, and the jumps in double layer parts are added in order to obtain correct solutions. To compute the stress components with higher accuracy, the derivatives of Stokes velocity are computed with corrections as shown in Section 3.2. This way, the forces at all points will be computed with uniform accuracy. Then the flow is computed throughout the domain as before. Again, we see the errors advancing from first order to second in δ when using corrections. Using parameter values from the previous example, two-norms of these errors for different values of δ are given in Figs. 17 and 18.

Fig. 19 shows the matrix condition numbers. In the coupled case, the matrix is not symmetric, and we use an iterative scheme like GMRES to solve it. The matrix is mostly dense and includes the coefficients of both Stokes and Darcy forces **f** and **g** that come from evaluating different flow quantities. The rows corresponding to the interface points are fully dense, with the first half columns being the coefficients of Stokes forces **f** and the rest being the coefficients of Darcy forces **g**. For example, for the first component of Stokes velocity u in the uncorrected case, the ith row of the system has the following expression:

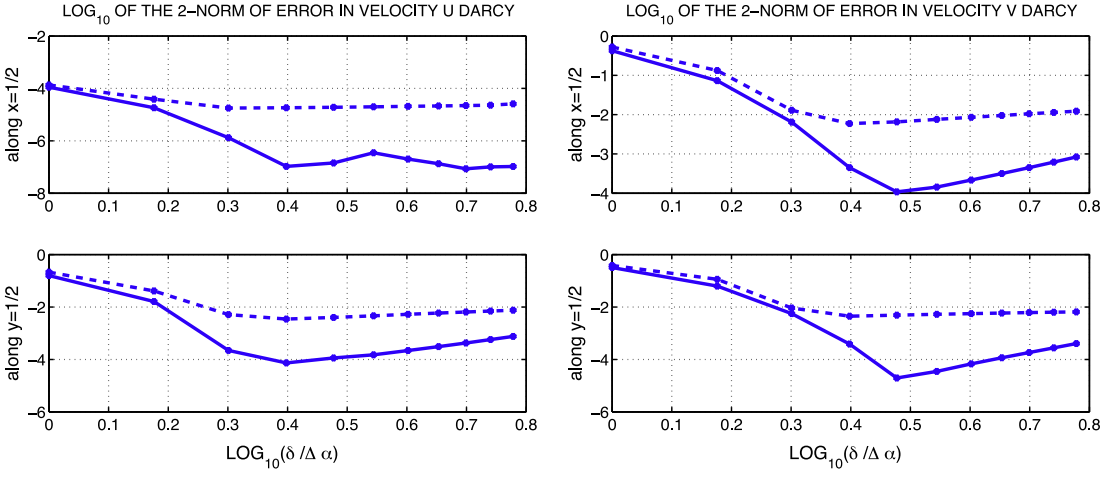

Fig. 17. Coupled solution: two-norm error in Darcy velocities u (left) and v (right) along different lines (dashed – uncorrected, solid – corrected).

Please cite this article in press as: S. Tlupova, R. Cortez, Boundary integral solutions of coupled Stokes and Darcy flows, J. Comput. Phys. (2008), doi:10.1016/j.jcp.2008.09.011

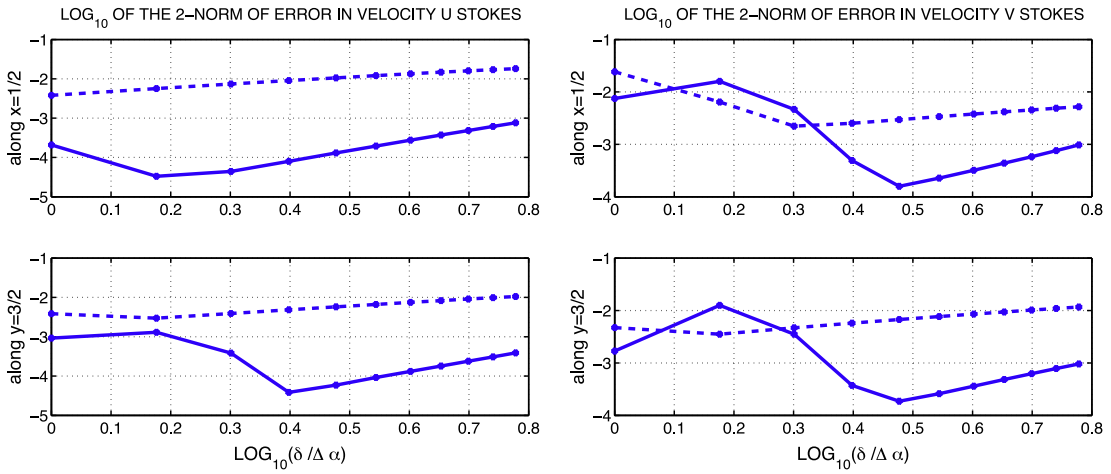

Fig. 18. Coupled solution: two-norm error in Stokes velocities u (left) and v (right) along different lines (dashed – uncorrected, solid – corrected).

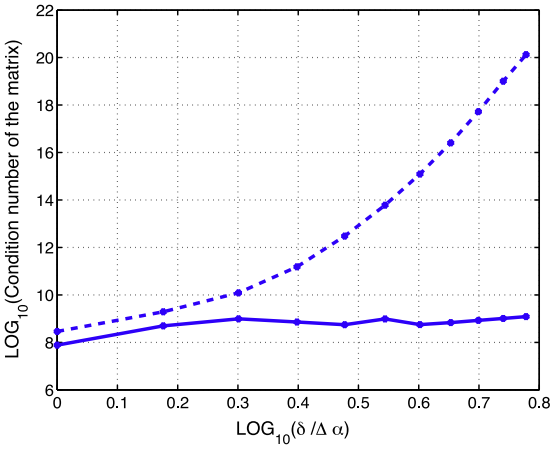

Fig. 19. Coupled solution: matrix condition numbers (dashed – uncorrected, solid – corrected).

$$\mu u^{\delta}(\mathbf{x}_i) = \sum_{k=1}^{N} f_k^1 M_\delta^1(\mathbf{x}_i - \mathbf{x}_k) + \sum_{k=1}^{N} f_k^2 M_\delta^2(\mathbf{x}_i - \mathbf{x}_k) = \sum_{\substack{k=1 \\ k\neq i}}^{N} f_k^1 M_\delta^1(\mathbf{x}_i - \mathbf{x}_k) + \sum_{\substack{k=1 \\ k\neq i}}^{N} f_k^2 M_\delta^2(\mathbf{x}_i - \mathbf{x}_k) + f_i^1 M_\delta^1(0) + f_i^2 M_\delta^2(0),$$

whereas in the corrected case the matrix elements become

$$\mu U^{\delta}(\mathbf{x}_i) = \sum_{\substack{k=1 \\ k\neq i}}^{N} f_k^1 M_\delta^1(\mathbf{x}_i - \mathbf{x}_k) + \sum_{\substack{k=1 \\ k\neq i}}^{N} f_k^2 M_\delta^2(\mathbf{x}_i - \mathbf{x}_k) + f_i^1 M_\delta^1(0) + f_i^2 M_\delta^2(0) + f_i^1 \mathrm{Correction}_\delta^1(0) + f_i^2 \mathrm{Correction}_\delta^2(0).$$

Here $u^{\delta}(\mathbf{x}_i) = U^{\delta}(\mathbf{x}_i) = u_{\mathrm{exact}}(\mathbf{x}_i)$ is the given velocity at the boundary point $\mathbf{x}_i$. Notice that the coefficients of f_i are the diagonal elements in the matrix. Adding the $\mathrm{Correction}_\delta(0)$ to these diagonal values keeps the condition number of the matrix bounded, therefore providing faster convergence of the iterative scheme. The condition numbers in the uncorrected case (dashed line in Fig. 19) grow exponentially(!) as δ grows for a fixed discretization size Δs. Making the discretization more dense for a fixed regularization will have the same effect.

5. Conclusions

We have presented a numerical method for computing accurate solutions of coupled Stokes and Darcy's equations. The method assumes the boundary integral formulation for both flows. The traditional approach is based on regularizing the singular integrands and approximating the integrals by a simple quadrature. On an example of a translating sphere in three dimensions, we showed that application of this method to boundary value problems results in low accuracy of the solutions.

Please cite this article in press as: S. Tlupova, R. Cortez, Boundary integral solutions of coupled Stokes and Darcy flows, J. Comput. Phys. (2008), doi:10.1016/j.jcp.2008.09.011

In the present work, the error due to regularization is corrected to the next order of accuracy. The singular integrals for Darcy and Stokes pressure, velocity, and velocity gradients in two dimensions are reformulated as single and double layer potentials. This allows the modifications to be more general and less geometry dependent. The numerical error then consists of error due to regularizing these potentials and then applying a standard discretization procedure. The regularization error is reduced by eliminating its largest term.

Various test cases were presented to show that results are consistent with theoretical predictions. In the first example, we computed Stokes flow in a channel driven by a uniform pressure gradient. Assuming the lower boundary as a porous boundary and assigning the slip boundary condition of Beavers–Joseph–Saffman gives a velocity profile that is non-zero at that boundary. Using corrected expressions, the slip velocity was calculated more accurately than with uncorrected expressions. The error as a function of regularization parameter δ reduces in magnitude and convergence increases from $O(\delta)$ to $O(\delta^2)$ with our method.

We tested the Darcy solution by prescribing an exact velocity on a circle. The kernels in the Darcy velocity have singularities of higher order, and we observe numerical errors in the uncorrected case as large as 20% in velocity and 70% in pressure. The corrections reduce the error by high factors of 100–1000, and accuracy increases by one order. Also, we compared results obtained using a trapezoidal rule and a four-point Gaussian quadrature. This affects the error due to discretization, which is most dominant for small regularization δ. For large values of δ using a more accurate quadrature has negligible effect.

We applied the method to coupled problems and observed similar results. Using corrections reduces the errors by large factors. Also, the interface boundary conditions are satisfied with smaller errors.

The formulation of the method makes it general enough to be applied to any solutions of linear PDEs which can be represented as potentials. In this case, it is easier to address the error due to discretization and decrease the regularization error further. For potentials with given densities correction terms were derived by Beale and Lai [5] to increase the order of discretization and regularization errors from $O(h)$ and $O(\delta^2)$ to $O(h^2)$ and $O(\delta^3)$, respectively. An exponential regularization factor was used in those calculations. Corresponding correction terms for our regularization can be derived easily. Applying these corrections will give regularization errors of $O(\delta^3)$, so it will be important to correct the discretization error as well.

This method can be applied to other singular solutions of Stokes flow, like dipoles and rotlets, since they are derived by differentiating the Stokeslet. The Darcy velocity, for example, is a dipole. This procedure can also be used to compute stresses in Stokes flow, since the velocity gradients are now computed with high accuracy. When using the uncorrected expressions, the jump across the boundary in the double layer potential has to be included into account for correct solution. Adding correction terms eliminates this need.

The equations we solve are steady state, but once the fluid velocity is known, the positions of the Lagrangian particles can be updated in time, thus extending the method to time-dependent problems.

Acknowledgments

This research was supported in part by NSF Grants DMS-0094179 and DMS-0612625, and by a Louisiana EPSCoR LINK program.

References

[1] J. Ainley, S. Durkin, R. Embid, P. Boindala, R. Cortez, The method of images for regularized Stokeslets, J. Comput. Phys. (2008), doi:10.1016/j.jcp.2008.01.032.
[2] P.J. Alvarez, W.A. Illman, Bioremediation and Natural Attenuation: Process Fundamentals and Mathematical Models, Wiley Interscience, 2006.
[3] J.T. Beale, A convergent boundary integral method for three-dimensional water waves, Math. Comp. 70 (2001) 977–1029.
[4] J.T. Beale, A grid-based boundary integral method for elliptic problems in three dimensions, SIAM J. Numer. Anal. 42 (2001) 599–620.
[5] J.T. Beale, M.-C. Lai, A method for computing nearly singular integrals, SIAM J. Numer. Anal. 38 (2001) 1902–1925.
[6] J.T. Beale, A.T. Layton, On the accuracy of finite difference methods for elliptic problems with interfaces, Commun. Appl. Math. Comput. Sci. 1 (2006) 91–119.
[7] J. Bear, A. Verruijt, Modeling Groundwater Flow and Pollution, Riedel Publ., 1987.
[8] G.S. Beavers, D.D. Joseph, Boundary conditions at a naturally permeable wall, J. Fluid Mech. 30 (1967) 197–207.
[9] D.M. Broday, Motion of nanobeads proximate to plasma membranes during single particle tracking, Bull. Math. Biol. 64 (2002) 531–563.
[10] E. Burman, P. Hansbo, A unified stabilized method for Stokes' and Darcy's equations, J. Comput. Appl. Math. 198 (2007) 35–51.
[11] A.T. Chwang, T.Y.-T. Wu, Hydromechanics of low-Reynolds-number flow, Part 2, Singularity method for Stokes flows, J. Fluid Mech. 67 (1975) 787–815.
[12] L. Cisneros, R. Cortez, C. Dombrowski, R. Goldstein, J. Kessler, Fluid dynamics of self-propelled micro-organisms, from individuals to concentrated populations, Exp. Fluids 43 (2007) 737–753.
[13] D. Colton, R. Kress, Inverse Acoustic and Electromagnetic Scattering Theory, 2nd ed., Springer-Verlag, Berlin, 1998.
[14] R. Cortez, The method of regularized Stokeslets, SIAM J. Sci. Comput. 23 (4) (2001) 1204–1225.
[15] R. Cortez, L. Fauci, A. Medovikov, The method of regularized Stokeslets in three dimensions: analysis, validation, and application to helical swimming, Phys. Fluids 17 (2005) 1–14.
[16] P. Daripa, D. Palaniappan, Singularity induced exterior and interior Stokes flows, Phys. Fluids 13 (11) (2001) 3134–3154.
[17] M. Discacciati, E. Miglio, A. Quarteroni, Mathematical and numerical models for coupling surface and groundwater flows, Appl. Numer. Math. 43 (2002) 57–74.
[18] L. Elasmi, F. Feuillebois, Green function for a Stokes flow near a porous slab, Z. Angew. Math. Mech. 81 (11) (2001) 743–752.
[19] H. Flores, E. Lobaton, S. Méndez-Diez, S. Tlupova, R. Cortez, A study of bacterial flagellar bundling, Bull. Math. Biol. 67 (2005) 137–168.
[20] J. Galvis, M. Sarkis, Balancing domain decomposition methods for mortar coupling Stokes–Darcy systems, Lecture notes in Computational Science and Engineering, 2006.
[21] J.K. Guest, J.H. Prevost, Topology optimization of creeping fluid flows using a Darcy–Stokes finite element, Int. J. Numer. Meth. Eng. 66 (2006) 461–484.

Please cite this article in press as: S. Tlupova, R. Cortez, Boundary integral solutions of coupled Stokes and Darcy flows, J. Comput. Phys. (2008), doi:10.1016/j.jcp.2008.09.011

[22] N. Hanspal, A. Waghode, V. Nassehi, R. Wakeman, Numerical analysis of coupled Stokes/Darcy flows in industrial filtrations, Trans. Porous Med. 64 (2006) 73–101.
[23] J.J.L. Higdon, The generation of feeding currents by flagellar motions, J. Fluid Mech. 94 (1979) 305–330.
[24] J.J.L. Higdon, A hydrodynamic analysis of flagellar propulsion, J. Fluid Mech. 90 (1979) 685–711.
[25] W. Jager, A. Mikelić, On the interface boundary condition of Beavers, Joseph, and Saffman, SIAM J. Appl. Math. 60 (2000) 1111–1127.
[26] J.B. Keller, S.I. Rubinow, Slender-body theory for slow viscous flow, J. Fluid Mech. 75 (1976) 705–714.
[27] R. Kress, Linear Integral Equations, 2nd ed., Springer-Verlag, New York, 1999.
[28] W.J. Layton, F. Schieweck, I. Yotov, Coupling fluid flow with porous media flow, SIAM J. Numer. Anal. 40 (6) (2003) 2195–2218.
[29] J. Lighthill, Mathematical Biofluid Dynamics, SIAM, Philadelphia, 1975.
[30] J. Lighthill, Flagellar hydrodynamics, SIAM Rev. 18 (1976) 161–230.
[31] J. Lighthill, Helical distributions of Stokeslets, J. Eng. Math. 30 (1996) 35–78.
[32] N. Liron, S. Mochon, Stokes flow for a Stokeslet between two parallel flat plates, J. Eng. Math. 10 (1976) 287–303.
[33] K.A. Mardal, X.-C. Tai, R. Winther, A robust finite element method for Darcy–Stokes flow, SIAM J. Numer. Anal. 40 (2002) 1605–1631.
[34] A. Masud, T.J.R. Hughes, A stabilized mixed finite element method for Darcy flow, Comput. Meth. Appl. Mech. Eng. 191 (2002) 4341–4370.
[35] A. Mayo, The fast solution of Poisson's and the Biharmonic equations on irregular regions, SIAM J. Numer. Anal. 21 (2) (1984) 285–299.
[36] O.M. Phillips, Flow and Reactions in Permeable Rocks, Cambridge University Press, Cambridge, 1991.
[37] C. Pozrikidis, Boundary Integral and Singularity Methods for Linearized Viscous Flow, Cambridge University Press, Cambridge, 1992.
[38] C. Pozrikidis, On the transient motion of ordered suspensions of liquid drops, J. Fluid Mech. 246 (1993) 301–320.
[39] C. Pozrikidis, Introduction to Theoretical and Computational Fluid Dynamics, Oxford University Press, Oxford, 1997.
[40] C. Pozrikidis, D.A. Farrow, A model for fluid flow in solid tumors, Ann. Biomed. Eng. 31 (2003) 181–194.
[41] G.P. Raja Sekhar, T. Amaranath, Stokes flow inside a porous spherical shell, Z. Angew. Math. Phys. 51 (2000) 481–490.
[42] P.G. Saffman, On the boundary condition at the surface of a porous medium, Stud. Appl. Math. L 2 (1971) 93–101.
[43] L.F. Shatz, Singularity method for oblate and prolate spheroids in Stokes and linearized oscillatory flow, Phys. Fluids 16 (3) (2004) 664–677.
[44] S. Tlupova, Improved Accuracy of Numerical Solutions of Coupled Stokes and Darcy Flows Based on Boundary Integrals, Ph.D. Thesis, Tulane University, 2007.
[45] G.A. Truskey, F. Yuan, D.F. Katz, Transport Phenomena in Biological Systems, Prentice Hall, 2003.

Please cite this article in press as: S. Tlupova, R. Cortez, Boundary integral solutions of coupled Stokes and Darcy flows, J. Comput. Phys. (2008), doi:10.1016/j.jcp.2008.09.011